



# **POLITECNICO DI TORINO**

---

DEPARTMENT OF MECHANICAL AND AEROSPACE ENGINEERING

Master of Science in Aerospace Engineering

## **Development of a telecommunication payload for light stratospheric platforms**

### **Supervisors**

Prof. Giorgio GUGLIERI

Dott. Victor MIHEREA

Dott. Gabriele SARTOR

### **Candidate**

Luca PACE

April 2021



## **Abstract**

High Altitude Platforms Stations (HAPS) are an enabling technology that could respond to the increasing demand for connectivity that the world is experiencing. This thesis, realised in collaboration with Stratobotic s.r.l., a startup founded in Turin focused on such services, is aimed at developing a lightweight, low power and re-configurable telecommunication payload to deliver scalable solutions.

A series of telecommunication links, in which HAPS could play a significant role, are evaluated and analysed in the form of Link Budgets.

Functional and physical designs are also developed and investigated, analysing the performances of the payload with MATLAB/Simulink.

In the last part of the thesis, a commercial transceiver for high-throughput (25Mbps) applications is tested and LOS communication links are established on ground to collect payload and telemetry data in real time.

# Table of Contents

Abstract.....	iii
Table of Contents .....	iv
Figures.....	vi
Tables.....	vii
Definitions and abbreviations .....	viii
1 Introduction.....	1
1.1 Context.....	1
1.2 New telecom trends and the ambition of global coverage .....	2
1.3 Scope and Objectives.....	3
1.4 State of the art of telecommunication HAPS.....	3
1.5 Regulations.....	4
1.5.1 <i>Aviation Regulation</i> .....	4
1.5.1 <i>Radio Spectrum Regulation</i> .....	6
2 Network Architecture .....	8
2.1 Preliminary considerations .....	8
2.1.1 <i>Basics of the stratospheric communication link</i> .....	8
2.1.2 <i>Operating frequency</i> .....	10
2.1.3 <i>Coverage</i> .....	11
2.2 Bidirectional FDD channel in C band .....	13
2.2.1 <i>Scenario and frequency planning</i> .....	13
2.2.2 <i>Link budget</i> .....	14
2.2.3 <i>Performances of the link</i> .....	15
2.3 Converging network with GEO satellites .....	18
2.3.1 <i>Scenario and frequency planning</i> .....	18
2.3.2 <i>Link budget</i> .....	20
2.3.3 <i>Performances of the link</i> .....	22
3 Advanced Payload Functional Design and Physical Baseline.....	24
3.1 Key drivers.....	24
3.2 Elements of a telecommunication payload .....	24
3.2.1 <i>Radiating elements</i> .....	25
3.2.2 <i>Receiver</i> .....	26
3.2.3 <i>Transmitter</i> .....	28
3.2.4 <i>Software Defined Radios</i> .....	29
3.3 Functional Baseline.....	30
3.4 Simulation .....	34
3.4.1 <i>Source and Channel</i> .....	35
3.4.2 <i>Receiver RF Front End</i> .....	35
3.4.3 <i>ADC and Digital Receiver</i> .....	37
3.4.4 <i>Output and Results</i> .....	37
4 Prototyping.....	40
4.1 Microhard pMDDL5824 .....	40
4.2 Preliminary configuration and testing.....	43
4.2.1 <i>Telemetry, Telecommand and Payload data stream</i> .....	43
4.2.2 <i>Short range test results</i> .....	48
4.3 Outdoor testing.....	51

4.3.1	<i>Selection of suitable antennas</i> .....	52
4.3.2	<i>Simulations</i> .....	56
5	Conclusions and future developments .....	60
	Bibliography .....	61

## Figures

Figure 1 AIRBUS Zephyr HAPS.....	1
Figure 2 Key ICT indicators for developed and developing countries, the world and special regions. Source: ITU World Telecommunication/ICT Indicators database. ....	2
Figure 3 Key ICT indicators by urban/rural area. Source: ITU World Telecommunication/ICT Indicators database.....	3
Figure 4 ICAO – ANNEX 2 Classification of unmanned free balloons.....	5
Figure 5 ITU regions and corresponding dividing lines .....	6
Figure 6 Free-space loss and gas attenuation for a typical HAPS operating at 20 km above the ground at different elevation angles. ....	9
Figure 7 Variation of a channel capacity with SNR and bandwidth .....	10
Figure 8 Received signal level on the ground for different geometric parameters and frequencies.....	11
Figure 9 Simulation of the coverage area that a HAPS at a 20 km altitude equipped with an 18° beamwidth, nadir pointing antenna would serve. Reported the -1, -2 and -3 dB levels relative to the maximum EIRP. ....	12
Figure 10 Performances of a standard parabolic reflector against diameter and frequency .....	12
Figure 11 SNR required for different order QAM .....	17
Figure 12 Ka-Sat spot beams.....	19
Figure 13 STK model: in cyan the satellite communication link, in purple the HAPS trajectory, in green the recovery link. Ship not in scale.....	20
Figure 14 Effect of rain and cloud fade on GEO Ka communication link .....	21
Figure 15 BER vs SNR for QPSK modulation.....	22
Figure 16 Example of a basic TDD RF transceiver configuration .....	24
Figure 17 Example of 3D directivity radiation pattern of a helical antenna at the centre frequency of 1.65 GHz.....	26
Figure 18 Simplified receiver diagram.....	26
Figure 19 Simplified transmitter diagram.....	28
Figure 20 HPA Pin/Pout transfer curve and Back-off operation .....	29
Figure 21 Components of a conceptual SDR. INSERT SOURCE .....	30
Figure 22 nuand bladeRF 2.0 microA9 block diagram.....	31
Figure 23 Simple 1x1 payload architecture .....	32
Figure 24 complete 2x2 payload architecture .....	33
Figure 25 Digital Receiver model in Simulink.....	35
Figure 26 Baseband Signal Generator in the Simulink model .....	35
Figure 27 Simulink Receiver RF Front End .....	36
Figure 28 Input Filter S21 parameter .....	36
Figure 29 Simulink Baseband Demodulator .....	37
Figure 30 Output spectrum of the simulation .....	38
Figure 31 Rx signal 16-QAM constellation at 20dB SNR.....	38
Figure 32 Simulation of the Bit Error Rate for a 16-QAM.....	39
Figure 33 pMDDL5824 operating modes.....	41
Figure 34 Setup to configure the Microhard transceiver via laptop.....	41
Figure 35 example of network status retrieving via Telnet.....	41
Figure 36 setup for telemetry and telecommand data exchange .....	43
Figure 37 TCP socket flow diagram .....	45
Figure 38 Receiving telemetry and payload data from the raspberry. ....	48
Figure 39 RF performances in short range test .....	49
Figure 40 Radiation pattern of a $\lambda/2$ 2.4 GHz whip antenna.....	52
Figure 41 Fade Margin variation with distance at 2.4 GHz in a 8MHz channel for the Microhard pMDDL5824 .....	53
Figure 42 Antenna alignment and misalignment for a point-to-point link using directional antennas .....	54
Figure 43 Examples of panel (a), Yagi (b) and Microstrip (c) antennas.....	55
Figure 44 Simulation of the outdoor test at Superga hill .....	56
Figure 45 Simulated results for a Superga-Turin link with Microhard pMDDL5824 using different antennas .....	58

## Tables

Table 1 ITU-R frequency allocation to HAPS services.....	7
Table 2 C band FDD link frequency planning .....	13
Table 3 FWD link budget - C band .....	14
Table 4 RTN link budget - C band .....	15
Table 5 FWD channel capacity .....	16
Table 6 QAM formats and comparison .....	17
Table 7 Throughput of FWD and RTN channels .....	18
Table 8 Ka-SAT 9A frequency plan for a blue spotbeam .....	19
Table 9 Number of users served by a beam of a GEO satellite operating in Ka band .....	23
Table 10 Payload budgets for different architectures .....	34
Table 11 Microhard pMDDL5824 performance specification @ maximum bandwidth and MIMO ON ....	40
Table 12 summary of request-reply pattern. In green compatible peer sockets, arrow indicates directionality of the pattern .....	46
Table 13 summary of publish-subscribe pattern. In green compatible peer sockets, arrow indicates directionality of the pattern. *allows to send/receive subscriptions .....	47
Table 14 summary of pipeline pattern. In green compatible peer sockets, arrow indicates directionality of the pattern. ....	47
Table 15 Microhard pMDDL5824 performance specification @ maximum bandwidth and MIMO OFF ...	57

## Definitions and abbreviations

ADC	Analogue to Digital Converter
AGI	Analytical Graphics, Inc.
APSK	Amplitude and Phase Shift Keying
AWGN	Additive White Gaussian Noise
BER	Bit Error Rate
BLOS	Beyond Line of Sight
CNR	Carrier to Noise Ratio
CPE	Customer Premises Equipment (serves fixed terminal links between HAPS and customer)
DSP	Digital Signal Processing
EIRP	Effective Isotropically Radiated Power
EVM	Error Vector Magnitude
FDM	Frequency Division Multiplexing
FEC	Forward Error Correction
FWD	Forward
FSL	Free-space Loss
GEO	Geosynchronous Earth Orbit
GPS	Global Positioning System
GSM	Global System for Mobile Communications
HTS	High Throughput Satellite
HPA	High Power Amplifier
IMU	Inertial Measurement Unit
ISR	Intelligence, Surveillance and Reconnaissance
LEO	Low Earth Orbit
LHCP	Left Hand Circular Polarization
LNA	Low Noise Amplifier
LOS	Line of sight
LTE	Long Term Evolution
MEO	Medium Earth Orbit
MIMO	Multiple Input Multiple Output
NFC	Near Field Communications
OS	Operating System
PFD	Power Flux Density
PIM	Passive Inter-Modulation
QAM	Quadrature Amplitude Modulation
RHCP	Right Hand Circular Polarization
RTN	Return
SATCOM	Satellite Communications
SDR	Software Defined Radio
SNR	Signal to Noise Ratio
S-PARAMETERS	Scattering Parameters
SSH	Secure Shell
STK	Systems Tool Kit
TCP	Transmission Control Protocol
TDD	Time-Division Duplexing
TRL	Technology Readiness Level
UAS	Unmanned Aircraft Systems

UAV	Unmanned Aerial Vehicle
UDP	User Datagram Protocol
WRC	World Radiocommunication Conference

# 1 Introduction

Since the early 1990s, several initiatives have been launched around the world to study and exploit the potential applications of high-altitude pseudo-satellites, also called High Altitude Platform Stations (HAPS). HAPS are aerospace vehicles able to fly above an altitude of 20 km in the stratosphere for months or even years, using their position to act as fixed platforms for a user on the ground. Some of the best candidates to accomplish these functions are proven to be stratospheric balloons, which have been widely used for meteorology so far. Planes and airships are viable candidates as well. Several HAPS development projects have recently reached more advanced stages of evolution, indicating that the first operations of such platforms could be expected in the near term.



Figure 1 AIRBUS Zephyr HAPS

## 1.1 Context

Looking at the world's satellite market it is possible to extrapolate some insights about the possible trend for the HAPS as the services that the latter are called to carry out are extremely comparable.

In the past decade, an increasing interest in small platforms has shown in the investors. The fast-changing needs of the users on the ground dictated the development of a new approach to space that can be translated to fast design, prototyping and launch.

The change in paradigm introduced in the space industry by the multiplication of satellites with a launch mass under 50 kg, as well as the deployment of mega-constellations, has started to revolutionize satellite design, testing and production. Manufacturers of big platforms are trying to find a way to reorganize their capabilities towards more rapid, simplified systems.

In addition to that, there is a continuous flurry of emerging space start-ups and this is generating an increasing interest amongst investors.

Differently from the 1990s, nowadays the growing interest in lowering the technology cost and development time could be a breeding ground to deliver observation, navigation, surveillance and communication services via HAPS.

Many investors have already started studies, technological demonstrations and first operations of such platforms. The applications of HAPS are now estimated to be multiple and such platforms could inaugurate a variety of opportunities and benefits to companies and users.

In short, HAPS could potentially act as enablers of more integrated services to a broader public.

## 1.2 New telecom trends and the ambition of global coverage

Telecommunications evolved rapidly in the last years, with the main focus being the increase of throughput, the reduction of the cost per bit and the implementation of seamless mobility. This trend had a large impact on both the ground communication market and the satellite communication market, breaking the balance that was created as yet.

Ground infrastructure technology improved consistently since the release of the ITU-R Recommendations: advancements in radio technology such as multi-carrier, MIMO and packet switching shaped the development of the LTE standard.

In the current context, the approach is changing from services to a multi-service approach. Pervasive network, group cooperative relay, cognitive radio technology, smart antennas are the main new technologies that are allowing the development of the 5G standard.

On the other side, the SATCOM technology evolved differently, as the increased competition in the downstream services produced uncertainty between operators. The demand for broadband changes more rapidly than the TV broadcast demand, moving the mix of customers that satellite operators now serve into less predictable territory.

Thus, flexibility and reconfigurability become exceptionally important for Telecommunication satellites manufacturers, with VHTS, being the most appealing solutions.

Satellite makers are opening to global, seamless and affordable connectivity solutions. The trend seems to be pointing to digital and integrated solutions, with software-defined satellites leading the scene.

Despite these efforts, at this moment, only about 50% of the world is connected, with huge disparities across regions. The reasons are multiple and amongst them surely it can be accounted for the lack of local infrastructures and the affordability of network services.

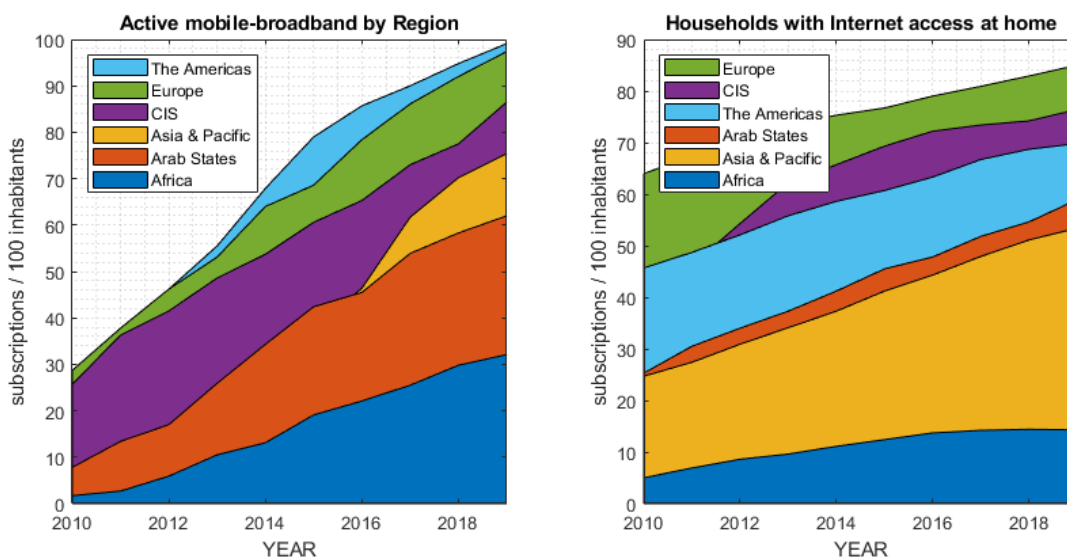
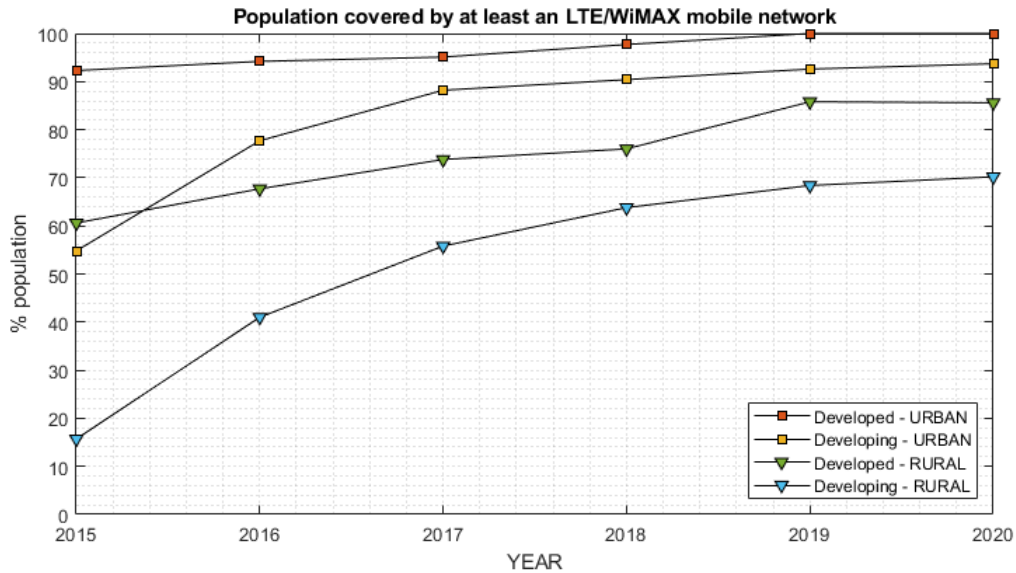


Figure 2 Key ICT indicators for developed and developing countries, the world and special regions.  
Source: ITU World Telecommunication/ICT Indicators database.



**Figure 3 Key ICT indicators by urban/rural area. Source: ITU World Telecommunication/ICT Indicators database.**

Even with the huge effort towards global connectivity made in the last years deploying the 5G standard, less than 34% of the population will have 5G coverage by 2025.

The 5G overarching ambition is to cover everything and everywhere, however, multiple users such as those in rural and suburban areas, aircraft and ships and other IoT devices will fall outside the range of terrestrial telecommunication systems.

### 1.3 Scope and Objectives

This thesis work summarises the studies and activities carried out with the start-up Stratobotic s.r.l.

Stratobotic aims to create working prototypes of HAPS for telecommunication and earth observation purposes by 2021. For this reason, the start-up hosted this graduation thesis which main goal is to provide RF analyses, individuate key parameters and, ultimately, design a payload that will demonstrate the capabilities of lightweight stratospheric balloons. In the last part of this thesis, support to a commercial transceiver that will be used in the first stages of testing is provided.

### 1.4 State of the art of telecommunication HAPS

Many are the advantages of bringing HAPS into the new radiocommunication scenario, being the natural complement to the existing non-terrestrial network composed of GEO, MEO and (V)LEO satellites.

Firstly, CAPEX and deployment complexity are extremely lower compared to the same figures for the satellite services. HAPS can be deployed quickly, on-demand and over any type of geography because minimal ground infrastructure is required. Furthermore, payloads can be

recovered and replaced at will, adding flexibility to the system and increasing its maintainability in case of a failure.

Secondly, HAPS could support low latency and stationary services much better than LEO's, providing spot capacity and offering wide cellular coverage in low-density areas. They could also share frequency spectrum with terrestrial cellular networks – Provided regulatory clearance and with interference control mechanisms.

There is a high variety of use-cases that can be imagined using an elevated base station serving directly users on the ground, extending from internet backhaul to IoT applications, this is demonstrated by the growing interests of companies that are aiming to develop concept and prototypes of such platforms:

- In 2013 AIRBUS Defence and Space purchased the Zephyr Project from QinetiQ. In July 2018, a Zephyr S, with a payload capacity of 5kg, flew in the stratosphere for nearly 26 days. Setting the record for the longest flight ever made without refuelling the aircraft. During the 2020 flight campaign - after two crashes happened in 2019 tests in Australia due to atmospheric turbulence – the aircraft operational flexibility and agility were demonstrated. AIRBUS aims to a full flight programme in 2021. Of note are the mass and power limitations on the payload for this aircraft model which makes it comparable to the stratospheric balloons.
- At Thales' Innovation Days, in 2014, the concept of an autonomous stratospheric airship, midway between a drone and a satellite, was presented. In 2016 the program was officially launched and in January 2020 Thales Alenia Space and Thales signed a contract with the French procurement agency to study applications of such platform in intelligence, surveillance and reconnaissance (ISR).
- In 2013 Google officially incubated a company whose main objective was to send small base stations in the stratosphere to provide connectivity to truckers and oil companies. Google began a test campaign with 30 stratospheric balloons to study the aerial network concept in June 2013. By July 2015, Google launched a mass-scale LTE service in Sri Lanka, then, in October 2017, 30 balloons were launched in Puerto Rico to provide emergency mobile coverage. Half a year later, Google claimed to have achieved a 155Mbps, stable, laser connection between two balloons over a distance of 100 km. After that, the company became an Alphabet subsidiary, named Loon. As of January 2021, Loon decided to shut down the company as the commercial viability of the project has proven harder than expected (Westgarth, 2021).

## **1.5 Regulations**

### **1.5.1 Aviation Regulation**

As per ICAO Annex 2 to the Convention on International Civil Aviation, a stratospheric balloon is defined as "Unmanned free balloon: A non-power-driven, unmanned, lighter than air aircraft in free flight."

These kinds of aerospace vehicles shall be classified as:

- a) light: a balloon with a payload, composed of one or more packages, with a cumulative mass of less than 4 kg.
  - b) medium: a balloon with a payload composed of two or more packages, with a cumulative mass between 4 and 6 kg.
  - c) heavy: a balloon with a payload with a cumulative mass of more than 6kg. To this category belong, as well, balloons that carry a payload with a mass of more than 2 kg and an area density of more than 13 g per square centimetre.
- Other payload configurations are classified as heavy, see Figure 4.

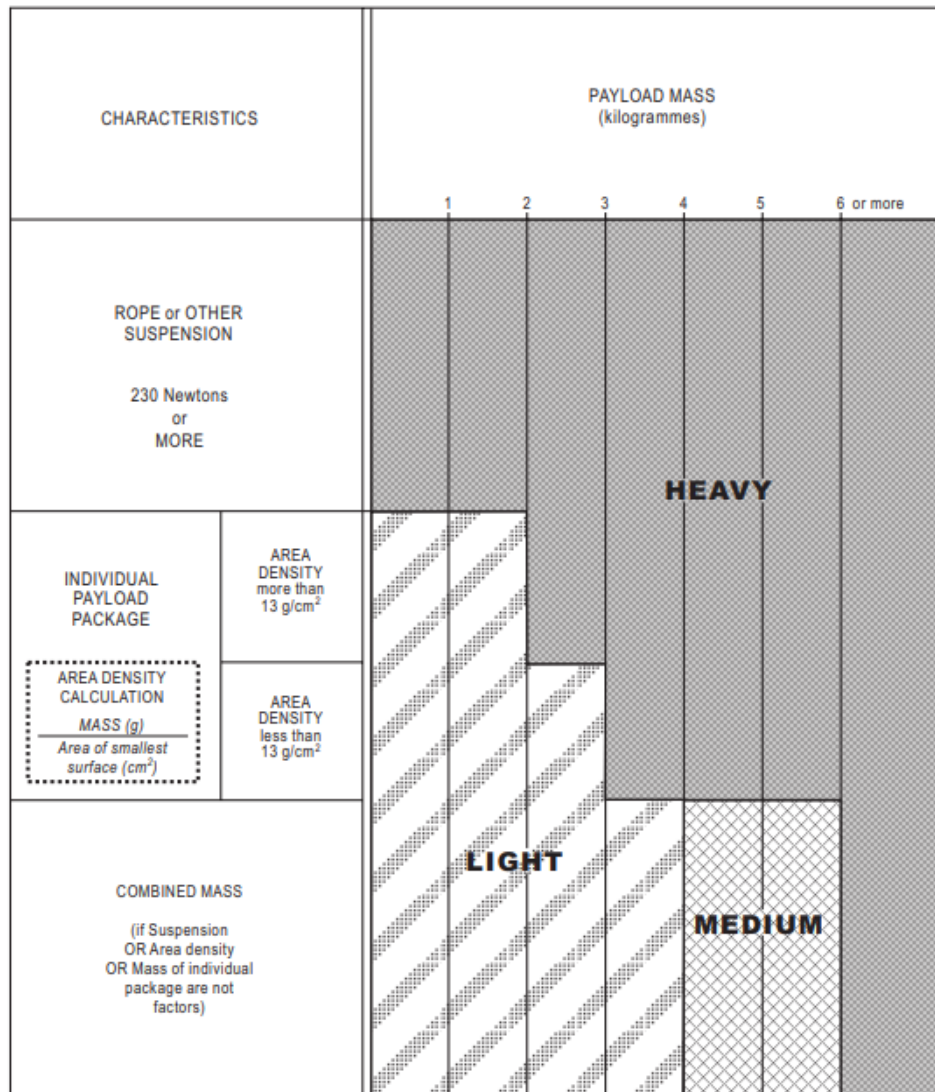


**Figure 4 ICAO – ANNEX 2 Classification of unmanned free balloons**

The Annex states also that the balloon shall be operated in such a way that hazards to people and other ground or air assets are minimized and gives a series of instructions to fly in compliance with safety and security standards.

This work focuses on light-type (a) balloons, as the overall process to obtain authorizations of flight from local authorities is ideal for the current objectives of Stratobotic S.r.l.

### 1.5.1 Radio Spectrum Regulation

The International Telecommunication Union is an agency of the United Nation that, throughout the ITU-R (Radiocommunication Sector) division it is responsible for the management of the international radio-frequency spectrum and satellite orbit resources.

In order to coordinate territorial frequency allocations ITU defines three regions:

- Region 1 comprises Europe, Africa, the former Soviet Union, Mongolia, and the Middle East west of the Persian Gulf, including Iraq.
- Region 2 covers the Americas including Greenland, and some of the eastern Pacific Islands.
- Region 3 contains most of non-FSU Asia east of and including Iran, and most of Oceania.

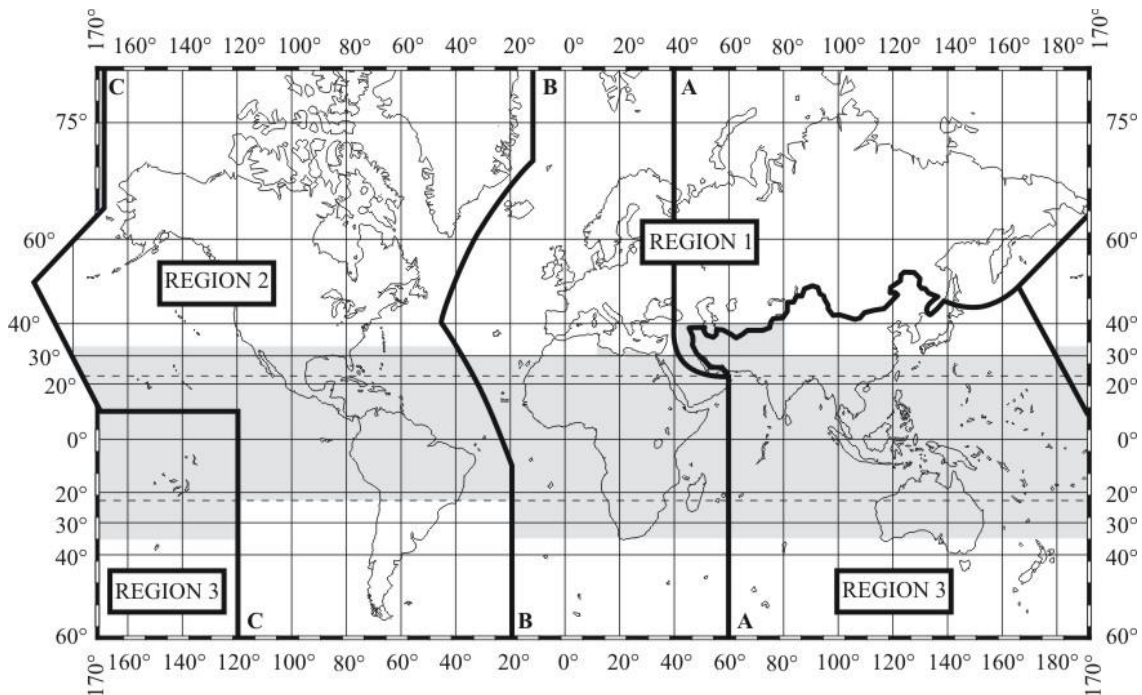


Figure 5 ITU regions and corresponding dividing lines

The ITU-R studies on spectrum needs for HAPS demonstrated that spectrum requirements for broadband HAPS applications may not be fully accommodated within previous HAPS identifications. Therefore, at WRC-19, delegates of ITU agreed on an extension of frequency bands for HAPS, which is shown in Table 1; arrows refer to Earth to HAPS ( $\uparrow$ ) or HAPS to Earth ( $\downarrow$ ) links. Naturally, the ITU in the WRC-19 Final Acts (International Telecommunication Union - Radiocommunication Sector, 2019), states PFD levels and other constraints that shall be considered.

Frequency band	Use	Direction	Bandwidth	Identification	
				Before WRC-19	After WRC-19
6 440-6 520 MHz	GW	↓	80 MHz	R1, R3	R1, R3
6 560-6 640 MHz	GW	↑	80 MHz	R1, R3	R1, R3
21.4-22 GHz	-	↓	600 MHz	-	R2
24.25-25.25 GHz	-	↓	500 MHz	-	R2
25.25- 27.0 GHz	GW for 25.5-27.0 GHz	↑	1500 MHz	-	R2
27.0-27.5 GHz	-	↓	500 MHz	-	R2
27.9-28.2 GHz	GW, CPE	↓	300 MHz	R1, R3	no change
31-31.3 GHz	GW, CPE	↑	300 MHz	R1, R3	Worldwide
38-39.5 GHz	-	↑↓	1500 MHz	-	Worldwide
47.2-47.5 GHz	GW, CPE	↑↓	300 MHz	Worldwide	Worldwide
47.9-48.2 GHz	GW, CPE	↑↓	300 MHz	Worldwide	Worldwide

**Table 1 ITU-R frequency allocation to HAPS services**

## 2 Network Architecture

In this chapter, simple communication links via HAPS are explained and engineering models in configurations of interest are evaluated and analysed.

### 2.1 Preliminary considerations

The objective of propagation modelling is often to determine the probability of satisfactory performance of a communication system or other system that depends on the propagation of electromagnetic signals. It is an essential factor to define a well-planned link budget. If modelling is too conservative, excessive costs may be incurred, while too lax modelling may lead to unsatisfactory performance. Therefore, the fidelity of the modelling must fit the intended application.

For network engineering, channel modelling consists of predicting the received signal strength at the end of the link and of estimating the capacity of the communication channel and its performances in various conditions. In fact, there are other channel disturbances that can degrade the performance of the link. These degradations include delay spreading (smearing in time) due to multipath and rapid fading of the signal within a symbol (distortion of the signal spectrum). These effects are usually considered to affect the equipment more than the communication link itself, so, for the purpose of this work, it is assumed that the hardware has been properly designed for the channel. In some cases, this may not be true and a communication link with sufficient receiving signal strength may not perform well.

Most of the propagation and link models in this thesis work are based on AGI Systems Tool Kit software, which allows customization and adaptation to ITU standard propagation models, fast link modifications, extensive data reporting and visualization. In general, it is a good idea to employ two or more independent models if they are available and to use the results as limits of expected performance.

#### 2.1.1 Basics of the stratospheric communication link

In this section, the basics of the link via HAPS will be covered. The essential parameters are the received signal strength, the noise accompanying the received signal, and any other channel degradation beyond attenuation, such as multipath or interference.

For link planning, a link budget is prepared taking into account the effective isotropically radiated power (EIRP) by the transmitter and all losses in the link before the receiver.

The link margin is obtained by comparing the expected received signal strength with the receiver sensitivity or threshold. The link margin is a measure of how much margin there is in the communication link between the operating point and the point at which the link can no longer be closed.

$$LinkMargin = EIRP - L_{Path} + G_{Rx} - MRS L_{Rx}$$

Where

$EIRP$  represents the effective isotropic radiated power by the transmitter in dBW or dBm

$L_{Path}$  is the total path loss, including miscellaneous losses, reflections, and fade margins in dB

$G_{Rx}$  is the receive gain in dB

$MRS L_{Rx}$  is the receiver minimum received signal level that will provide reliable operation (such as the desired bit error rate performance) in dBW or dBm

Many are the factors that can affect the link margin, including the type of modulation used, the transmitted power, the net gain of the antenna, any cable or ancillary loss between the transmitter and the antenna but, primary, path loss. In the path loss term are incorporated free-space loss, atmospheric losses due to gaseous and water vapour absorption, precipitation, fading loss due to multipath, and other miscellaneous effects based on the frequency and the environment.

Considering a HAPS floating at 20 km altitude, in clear sky, the main contributions to path loss are free-space loss (FSL), that can be expressed in dB as

$$L_{FSLdB} = -20 \log \left( \frac{\lambda}{4\pi d} \right)$$

and atmospheric attenuation.

Generally, atmospheric effects of interest for RF propagation are refraction/reflection, scattering, and absorption/attenuation, all of these are subject to frequency and geometry of the link. For HAPS links, atmospheric attenuation is the main source of loss of electromagnetic energy due to absorption from oxygen and water vapor. The absorption is generally described by a specific attenuation in dB/km for terrestrial paths and by a total attenuation as a function of elevation angle for slant paths that exit the troposphere.

In Figure 6 FSL and atmospheric attenuation is shown: it is clear that operating in the high part of the frequency spectrum will significantly affect the power requirements to provide sufficiently stable communication links.

In addition to these effects that are - to a certain extent- constant in time, three forms of variable atmospheric loss can significantly affect non-terrestrial communication links: precipitation, water vapour, and suspended water droplets, forming clouds or fog. Each depends on the local climate and its unique properties can affect electromagnetic waves differently. It is of interest

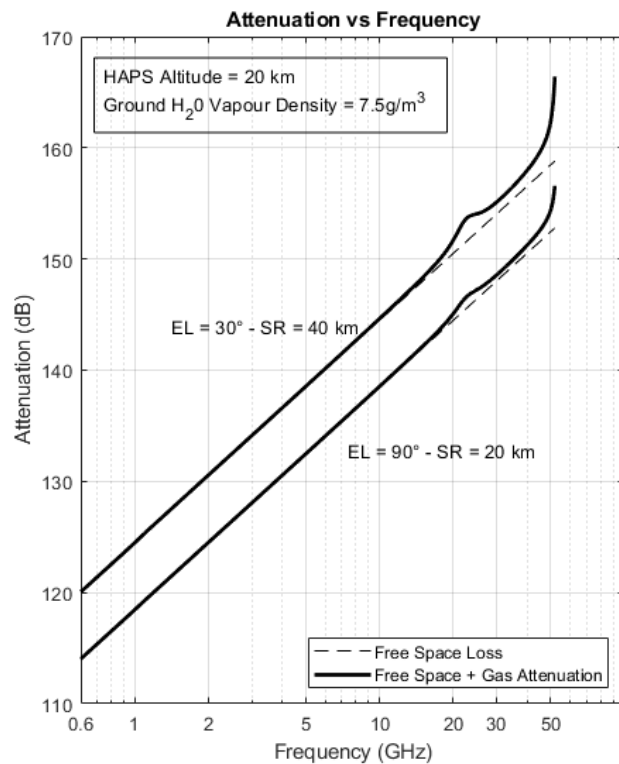


**Figure 6 Free-space loss and gas attenuation for a typical HAPS operating at 20 km above the ground at different elevation angles.**

to say that, rain attenuation will be a major challenge for HAPS operating in the millimetre wave spectrum (30 GHz or higher) as the loss due to rain could be as high as 10 dB or more for a HAPS located at 20 km in the sky and elevation angle of 30°, (ITU-R P.838-3, 2005).

For a more detailed explanation of such effects the reader can consult (Recommendations, ITU-R, 1999).

### 2.1.2 Operating frequency

As shown in the paragraph above, higher frequencies are related to higher path loss, however the higher frequencies benefit from not being overcrowded, therefore much greater bandwidth are available, which permits greater data flow and can reduce power requirements. This is a major advantage as bandwidth demands has increased to extreme levels in the last years, especially since the deployment of 5G services.

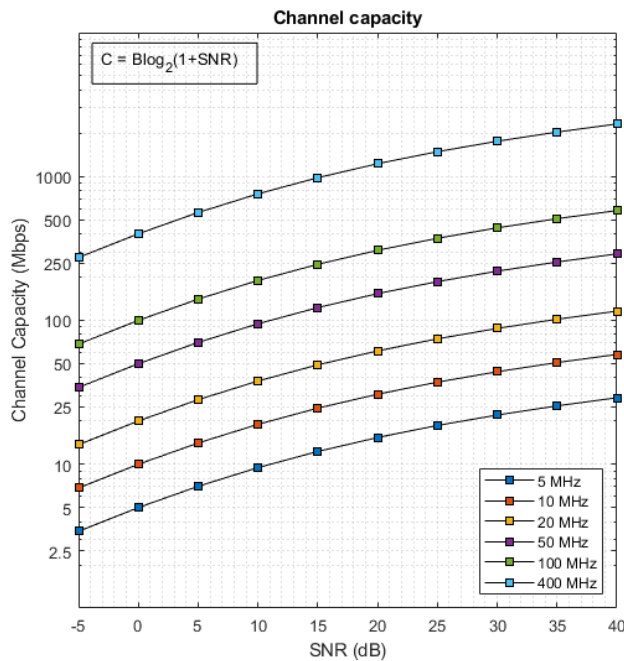


**Figure 7** Variation of a channel capacity with SNR and bandwidth

the channel capacity and it is a function of the spectral efficiency.

Higher frequencies also permit greater antenna gain for a given aperture size, or, at the contrary, allow smaller (and lighter) antennas given a certain antenna gain, that is a great advantage considering the tendency to operate with light platforms.

The upper limit to the information rate that can be transmitted over a communication channel in presence of noise is defined, essentially, by two main parameters that are the available bandwidth  $B$ , and the signal-to-noise ratio  $SNR$  (expressed as a linear power ratio). This is also known as the *Shannon-Hartley theorem*:

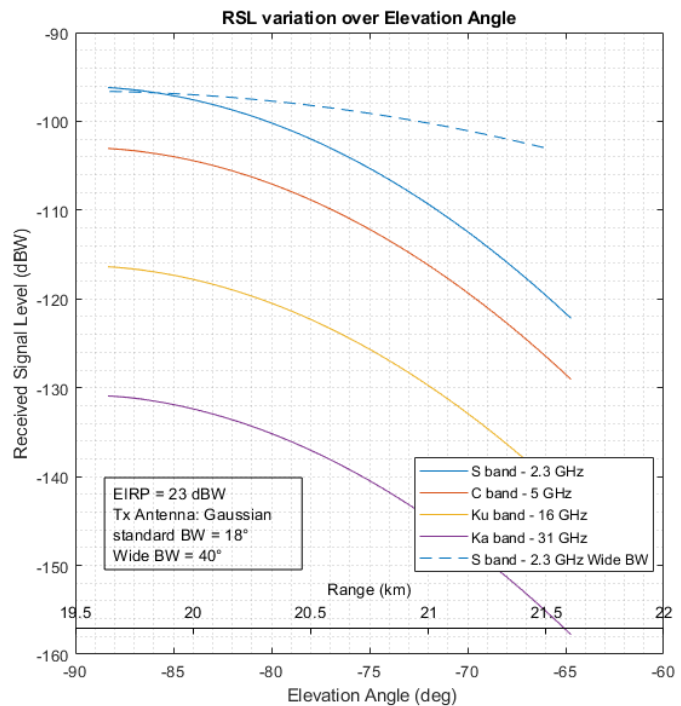
$$C = B \log_2(1 + S/N)$$

where  $C$  is the channel capacity in *bit/s*

The channel capacity will differ from the actual throughput of the communication channel. In particular, the throughput will always be less than

### 2.1.3 Coverage

As already said, given their lower distance from the ground, HAPS have a series of advantages compared to satellites: reduced network delay and increased signal to power ratios are some of them, nevertheless, they also suffer a reduced area of coverage. This is of noticeable importance because it will dictate a sets of constraints such as the maximum range and elevation angle with respect to the user, affecting the Guidance and Navigation system of the HAPS, its Attitude Determination System and its ability to, potentially, its tracking capabilities.



A typical service area for a platform located in the stratosphere could reach up to 80 kilometres in diameter. However, as the purpose of this work is to design a telecommunication payload for small and light HAPS, to serve such a wide area it would be too ambitious. A trade-off must be, therefore, evaluated considering onboard power, the number of radios, quantity and typology of the antennas etc.

Low gain antennas are useful to serve a broader region but might require a higher power to be installed onboard to have a satisfying EIRP in that area.

High gain, directive antennas can be considered for such applications where a strong RSL is needed without exceeding the HAPS power requirements, but this will reduce the area of coverage and expose the link to pointing errors, Figure 8.

As an example, given a HAPS at 20 km altitude equipped with a 18° beamwidth antenna, it would cover an area of about 3 km radius. That is almost as wide as the city of Turin, see Figure 9.

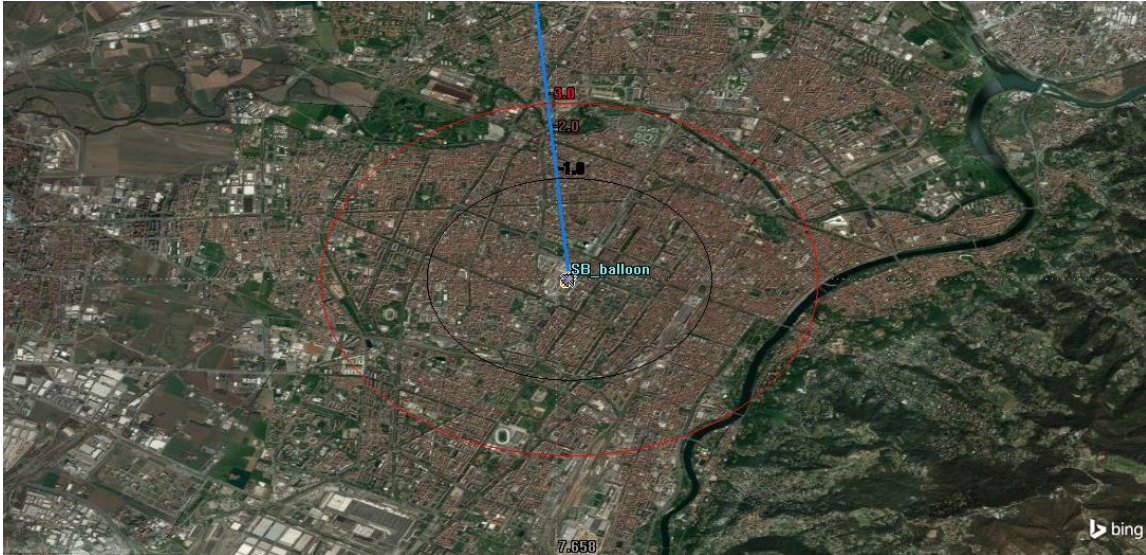


Figure 9 Simulation of the coverage area that a HAPS at a 20 km altitude equipped with an 18° beamwidth, nadir pointing antenna would serve. Reported the -1, -2 and -3 dB levels relative to the maximum EIRP.

To reach the desired coverage great attention should be pointed to the antenna design, which needs to be carefully selected (or designed for very specific missions), to match the desired application.

A wide range of antennas suitable for HAPS exists however, the higher the complexity, the lower it is the TRL it is. Generally, the technology spreads from simple patch antennas to parabolic reflectors and phased array able to support MIMO techniques.

Frequency also plays a key role in the selection of the right radiating element, as it will affect the geometry, therefore the weight of the component, see Figure 10.

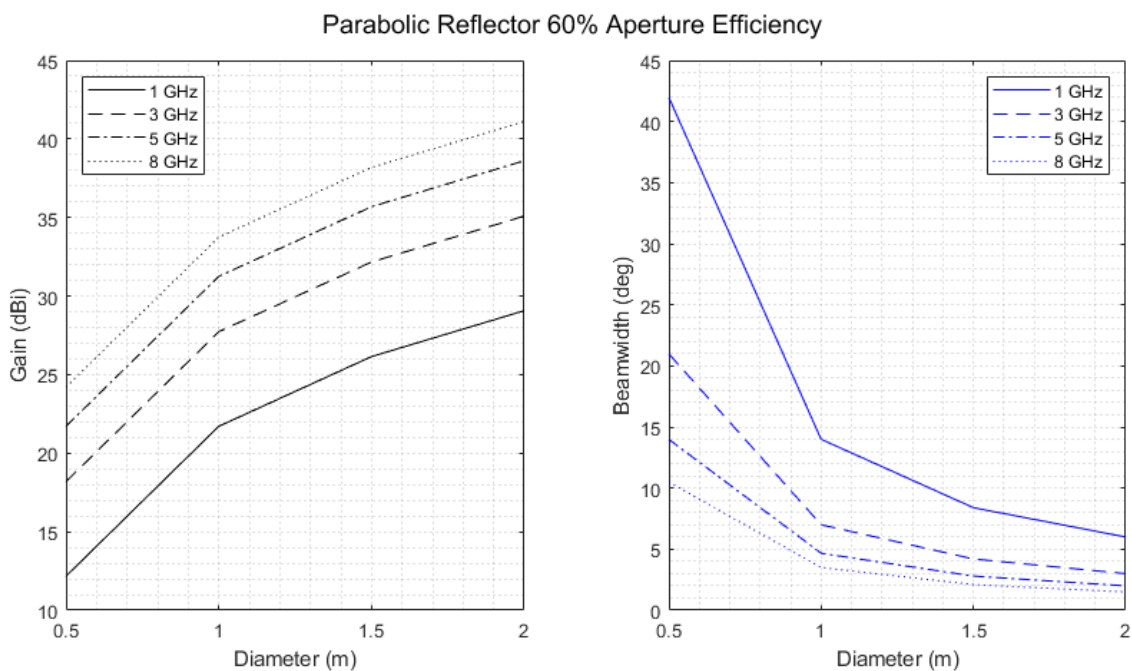


Figure 10 Performances of a standard parabolic reflector against diameter and frequency

## 2.2 Bidirectional FDD channel in C band

The simplest scenario that can be modelled to carry out some figures is a Point-to-Point/Point-to-Multipoint data relay link to re-transmit the information to users in a wireless network.

The real services this simple architecture could deliver are essentially BLOS communications or even LOS communication where constraints do not allow the deployment of ground infrastructure, such as unapproachable terrain or disaster assistance missions. Emergency communications, sport-events and large-scale broadcast services are some of the main uses of such a system.

However, extensive literature on this topic already exists, therefore a more complex architecture will be considered to start with.

As mentioned, the growing interest today is to connect everything and everywhere, therefore HAPS could give force to maritime connectivity, which, at the moment, is served only via satellite.

A Point-to-Point, bidirectional link is therefore modelled to deliver internet connectivity in a realistic scenario.

### 2.2.1 Scenario and frequency planning

The scenario consists of a single ship (user) cruising the Tyrrhenian Sea and a small Ground Station (gateway) placed on the Italian coast beyond the line of sight of the user. The distance between these two can potentially range from 50 to 350 kilometres but, to evaluate the worst-case scenario, a range that spans from 230 to 350 km is considered. A stratospheric balloon hovers on the midpoint between the GW and user at 20 km altitude and it is assumed to be able to track both.

The link consists of a bidirectional FDD channel, divided as follows:

Mission			Frequency [MHz]
FWD	<i>Uplink</i>	<i>GW → Balloon</i>	<i>5700 RHCP</i>
	<i>Downlink</i>	<i>Balloon → UE</i>	<i>5700 LHCP</i>
RTN	<i>Uplink</i>	<i>UE → Balloon</i>	<i>5800 RHCP</i>
	<i>Downlink</i>	<i>Balloon → GW</i>	<i>5800 LHCP</i>

**Table 2 C band FDD link frequency planning**

The reason to choose such frequencies is that C band has a portion of the spectrum allocated to amateur radio (IEEE, s.d.), therefore, at the beginning of the test phases, a prototype can easily be authorized to operate.

Given the low frequency, a low elevation angle is allowed. It should be noted that, in the case of higher frequencies, the elevation angle between user and balloon should be increased to at least 30 degrees.

## 2.2.2 Link budget

The link budget is evaluated with the following environmental considerations:

- Total propagation and rain loss calculation according to (ITU-R P.618, 2017)
- Clouds and fog model according to (ITU-R P840-6, 2013), liquid water content density of  $7.5g/m^3$ , cloud layer thickness of 500 m
- Simple atmospheric absorption model with water vapor concentration of  $7.5g/m^3$

Furthermore, for initial testing, it is supposed to assess the link performances with a simple ground station equipment, that is composed by 100 W (20 dBw) transmitter with a 30 cm parabolic reflector, that requires less precise balloon tracking.

On the balloon, given the constraints, low power (less than 5 W) and low gain reflector are imagined to be installed.

The User Equipment should be easily deployable and relieved from stringent power and size requirements; for now it is modelled as a 10 W radio equipped with a 60 cm parabolic reflector, however, for future developments and commercial viability, it should be considered to select a less directional antenna.

FWD Uplink		FWD Downlink	
<i>Transmitter</i>		<i>Transmitter</i>	
Transmitted Power	20 dBw	Transmitted Power	7 dBw
tx Antenna Diameter	30 cm	tx Antenna Diameter	30 cm
tx Antenna Gain	22.5 dBi	tx Antenna Gain	22.85 dBi
<b>EIRP</b>	<b>42.5 dBw</b>	<b>EIRP</b>	<b>29.85 dBw</b>
<i>Receiver</i>		<i>Receiver</i>	
rx Antenna Diameter	30 cm	rx Antenna Diameter	60 cm
rx Antenna Gain	22.8 dBi	rx Antenna Gain	28.9 dBi
<b>G/T</b>	<b>-7.45 dB/K</b>	<b>G/T</b>	<b>-5.4 dB/K</b>
<i>Losses</i>		<i>Losses</i>	
<b>Range</b>	<b>139 km</b>	<b>Range</b>	<b>140 km</b>
Free Space Loss	150 dB	Free Space Loss	150.5 dB
Atmospheric Loss	0.3 dB	Atmospheric Loss	0.3 dB
Rain Loss	1.1 dB	Rain Loss	1 dB
Cloud and Fog Loss	0.8 dB	Cloud and Fog Loss	0.9 dB
<b>Total Losses</b>	<b>153 dB</b>	<b>Total Losses</b>	<b>152.7 dB</b>
<i>Link Performance</i>		<i>Link Performance</i>	
C/N0	51.1 dB*MHz	C/N0	40.4 dB*MHz
<b>C/N</b>	<b>38.1 dB</b>	<b>C/N</b>	<b>27.4 dB</b>
<b>Eb/N0</b>	<b>35.2 dB</b>	<b>Eb/N0</b>	<b>24.4 dB</b>

Table 3 FWD link budget - C band

RTN Uplink		RTN Downlink	
<i>Transmitter</i>		<i>Transmitter</i>	
Transmitted Power	10 dBw	Transmitted Power	2 dBw
tx Antenna Diameter	60 cm	tx Antenna Diameter	30 cm
tx Antenna Gain	29.02 dBi	tx Antenna Gain	23 dBi
<b>EIRP</b>	<b>39.02 dBw</b>	<b>EIRP</b>	<b>25 dBw</b>
<i>Receiver</i>		<i>Receiver</i>	
rx Antenna Diameter	30 cm	rx Antenna Diameter	30 cm
rx Antenna Gain	23 dBi	rx Antenna Gain	23 dBi
<b>G/T</b>	<b>-7.3 dB/K</b>	<b>G/T</b>	<b>-6.63 dB/K</b>
<i>Losses</i>		<i>Losses</i>	
<b>Range</b>	<b>140 km</b>	<b>Range</b>	<b>138.8 km</b>
Free Space Loss	150.6 dB	Free Space Loss	150.6 dB
Atmospheric Loss	0.3 dB	Atmospheric Loss	0.3 dB
Rain Loss	0.8 dB	Rain Loss	0.6 dB
Cloud and Fog Loss	1 dB	Cloud and Fog Loss	0.8 dB
<b>Total Losses</b>	<b>152.7 dB</b>	<b>Total Losses</b>	<b>152.3 dB</b>
<i>Link Performance</i>		<i>Link Performance</i>	
C/N0	47.5 dB*MHz	C/N0	34.5 dB*MHz
<b>C/N</b>	<b>34.5 dB</b>	<b>C/N</b>	<b>21.5 dB</b>
<b>Eb/N0</b>	<b>31.5 dB</b>	<b>Eb/N0</b>	<b>18.5 dB</b>

Table 4 RTN link budget - C band

It is notable that the antenna gains, transmission losses and transmitted power all directly affect the link budget. In this case, the path loss is the most significant factor due to its magnitude compared to the other terms. At these frequencies atmospheric absorption and rain loss are mostly not relevant, however, as the frequency increases, it will not be possible to reach such performance figures with such coupling of geometry, power and gains.

### 2.2.3 Performances of the link

In 2.1.2 it is expressed the capacity of a communication channel given its signal quality (SNR, or CNR in case of the table above), this figure does not represent the actual data rate, it is rather an upper limit. In case of the FWD link, the channel capacity computed with the minimum CNR (27.4 dB) it is represented in Table 5 FWD channel capacity Table 5.

Channel Bandwidth	Channel Capacity
1 MHz	87.7 Mbps
5 MHz	438.5 Mbps
10 MHz	877.0 Mbps
20 MHz	1754.0 Mbps
50 MHz	4384.9 Mbps
100 MHz	8769.9 Mbps

300 MHz	26309.7 Mbps
---------	--------------

**Table 5 FWD channel capacity**

The real throughput of the channel is mainly dictated by the bandwidth, the channel utilization, and the spectral efficiency.

$$\text{Channel Throughput} = BW \times \text{Channel Utilization} \times \text{Spectral Efficiency}$$

where

- *Channel Throughput* is the channel effective bit rate in *bit/s*
- *BW* is the actual bandwidth in *Hz* excluding the used guard band
- *Channel Utilization* is the percentage of channel used
- *Spectral Efficiency* is the maximum achievable information rate of the considered modulation scheme which in the given noisy channel can be practically obtained when are applied symbol shaping and forward error correction. It is measured in *(bit/s)/Hz*

For a Point-to-Point communication link, as in this case, channel utilization can be considered 100%, but in general, this hypothesis does not hold in a Point-to-Multipoint network.

The bandwidth is the main degree of freedom in this analysis it will be the more flexible parameter that will dictate the total throughput.

Spectral efficiency is constrained by the link quality (SNR or  $E_b/N_0$ ), in this case, for simplicity, a digital modulation Quadrature amplitude modulation (QAM) is considered.

QAM modulates two carriers shifted in phase by 90 degrees in a condition of orthogonality or quadrature. This type of modulation, used for digital transmission, can deliver higher data rates than ordinary amplitude modulations or phase modulations, nevertheless, it is more susceptible to noise.

QAM assigns different positions on a constellation diagram to different digital values, in this way, two I and Q signals (“I” is the in-phase signal, while “Q” is the out of phase signal) can code different bits, the number of bits assigned depends on the order of the QAM adopted. In particular, constellations can contain points equal to powers of 2 (i.e. 4-QAM, 16-QAM, 64-QAM, 256-QAM, etc.); the higher the order, the higher the bits coded per point, therefore, the higher the spectral efficiency. (<https://www.electronics-notes.com>, s.d.)

The advantage of using such modulation is that the symbol rate can be adapted to the signal level by setting the appropriate constellation size that will affect the spectral efficiency.

Given the alphabet size which is formed by  $M$  symbols and  $N = \log_2(M)$ , the bit/symbol that the modulation allows. The spectral efficiency can be assumed equal to  $N$ , even though it should be considered that the use of error detection and correction schemes such as FEC will decrease the spectral efficiency but will increase the reliability of the channel.

Modulation	M	Spectral Efficiency (bit/s)/Hz
QPSK (equivalent to 4-QAM)	4	2
8PSK (equivalent to 8-QAM)	8	3
16QAM	16	4

32QAM	32	5
64QAM	64	6

**Table 6 QAM formats and comparison**

To select a suitable modulation that will achieve the highest data rates the key parameter is the BER (Bit Error Rate), which is the average number of bits received in error divided by the total number of bits received. Simple modulation schemes, like BPSK/QPSK, require less signal quality while links designed for ultra-high speeds will use a complex form of modulations that will require an excellent signal quality. (David Large, 2003)

Generally, a BER of  $10^{-6}$  is the upper limit of a reliable communication channel: the standard of acceptable BER in data communications ranges from  $10^{-9}$  to  $10^{-13}$ . In Figure 11 it is shown the theoretical SNR required for different modulation schemes to achieve such bit error rates in a channel in presence of AWGN.

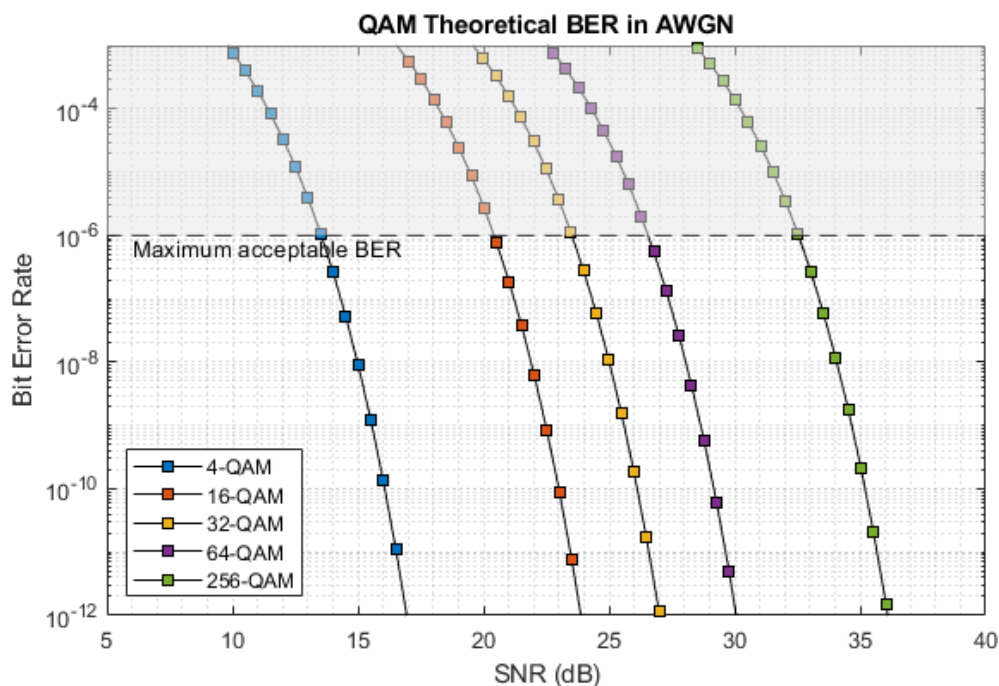


**Figure 11 SNR required for different order QAM**

As can be noted in Table 3, the minimum CNR in the FWD communication link is around 27.4 dB, therefore a 32-QAM modulation will be well supported by the link as it will provide a BER of less than  $10^{-12}$ ; a 64-QAM could be supported but the margin will be excessively tight. For the RTN channel, in Table 4 can be noted that the minimum CNR is 21.5 dB, that will provide a BER of  $10^{-8}$  with 16-QAM, again, to keep some margin, the best option is to consider a 8-PSK (or 8-QAM) modulation.

Once the suitable modulation scheme is chosen, the channel throughput can be calculated:

<b>Downlink 32-QAM</b>		<b>Uplink 8-QAM</b>	
<b>Channel Bandwidth</b>	<b>Channel Throughput</b>	<b>Channel Bandwidth</b>	<b>Channel Throughput</b>
1 MHz	5.0 Mbps	1 MHz	3.0 Mbps

5 MHz	25.0 Mbps	5 MHz	15.0 Mbps
10 MHz	50.0 Mbps	10 MHz	30.0 Mbps
20 MHz	100.0 Mbps	20 MHz	60.0 Mbps
50 MHz	250.0 Mbps	50 MHz	150.0 Mbps
100 MHz	500.0 Mbps	100 MHz	300.0 Mbps
300 MHz	1500.0 Mbps	300 MHz	900.0 Mbps

**Table 7 Throughput of FWD and RTN channels**

As stated before, these performances are valid for a Point-to-Point communication link that will require a good pointing system. In case of multiple users, a more advanced link budget shall be evaluated, considering that:

- The throughput will be split between the users
- The users may be a few kilometres apart

## **2.3 Converging network with GEO satellites**

Another useful scenario that can be analysed amongst many, is a cooperating mission with an existing network that is subject to sudden interruption of service.

In fact, light HAPS can be quickly deployed at need, improving the Network Resilience, that is the ability of the network to deliver and maintain an appropriate level of service in the face of various faults and challenges to normal operation.

This could be the case of satellite internet connection that is currently delivered only by GEO satellites, although SpaceX has already launched a beta test of its Starlink LEO internet services (Sheetz, 2020). To improve the capacity of the link, satellite transponders are shifting to higher frequencies, but as said in 2.1.1, higher frequencies are susceptible to rain and cloud loss, weakening the link availability. In such case, or in case of critical communication networks, HAPS can be used to mitigate the service disruption, providing a fast recovery of the link.

Therefore, it is of interest to analyse the potential that HAPS could have in a real scenario, such as internet services delivered via satellite in higher bands of the spectrum, which suffer severe rain attenuation. In the Mediterranean basin one of the most recent services that were activated, is Tooway. But, over the Mediterranean, maritime thunderstorms can happen, and these are related with high durations that exceed 100 minutes (E. Galanaki, 2018): that would severely affect the performances of a communication link. Therefore, a realistic scenario to recover Tooway's communication link is modelled using STK.

### **2.3.1 Scenario and frequency planning**

At the moment, Eutelsat is using Ka-band capacity for a consumer broadband service, launched in Europe at the end of 2010, and called Tooway (Eutelsat Archived Communications, 2008). Tooway commercial services are delivered through the EUTELSAT Ka-SAT 9A, (now being acquired by Viasat (Werner, 2020)). The service is operated by the Group's broadband subsidiary Skylogic, in cooperation with ViaSat.

One of the ground stations that could be used by the company as Gateway is the Macchiareddu platform, located in the industrial area near Cagliari, however, for the purpose of this study, any ground station in the Skylogic loop could be used.

The Ka-SAT 9A is modelled as a simple geostationary satellite holding the 9E point. The orbit is propagated over 1 day with a J2Perturbation model; however, no orbital perturbation is expected to be significant in this scenario.

The user is represented by a stationary commercial ship in the Mediterranean Sea.

The model link is structured as follows: a forward mission Gateway → Ka-SAT 9A → User and a return mission User → Ka-SAT 9A → Gateway.

The Ka-Sat delivers data links through 82 spot beams to increase frequency reuse. Each of the spot beams has a coverage of around 250km of radius. Unfortunately, this is accomplished via a complex antenna design process. For the analysis in consideration, coverage is not the primary issue, therefore, a simple parabolic antenna of 3 m diameter is assumed to model one of the spot beams.

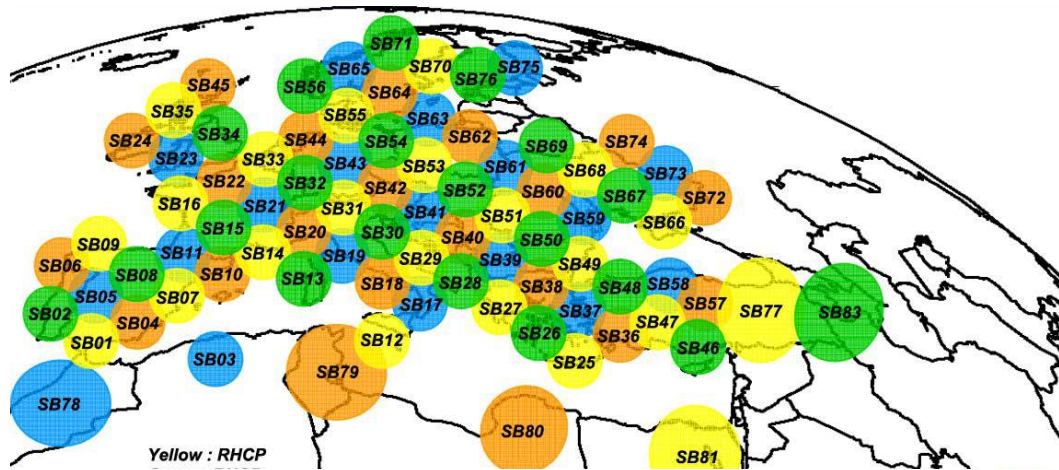


Figure 12 Ka-Sat spot beams

The transceivers proprieties are set considering a blue spotbeam, as per Ka-Sat frequency plan ([frequencyplansatellites.altervista.org](http://frequencyplansatellites.altervista.org)):

Mission			Frequency [MHz]	Polarization
FWD	Uplink	GW → Ka-SAT 9A	28963,75	RHCP
	Downlink	Ka-SAT 9A → UE	19818,75	LHCP
RTN	Uplink	UE → Ka-SAT 9A	29618,75	RHCP
	Downlink	Ka-SAT 9A → GW	19293,75	LHCP

Table 8 Ka-SAT 9A frequency plan for a blue spotbeam

The UE proprieties are set referencing with the ViaSat SurfBeam® 2 terminal guide, that indicates a Tx power of around 220 W, a parabolic reflector of 75 cm and the minimum quality of signal required.

A HAPS will be used to recover the communication link when the environmental conditions will degrade the satellite link performances (Figure 13 STK model: in cyan the satellite communication link, in purple the HAPS trajectory, in green the recovery link. Ship not in scale. Figure 13).

In particular, it will be used to recover the RTN uplink channel, therefore it will operate as a repeater for the 29618,75 MHz RHCP channel that will be attenuated by rain and clouds.

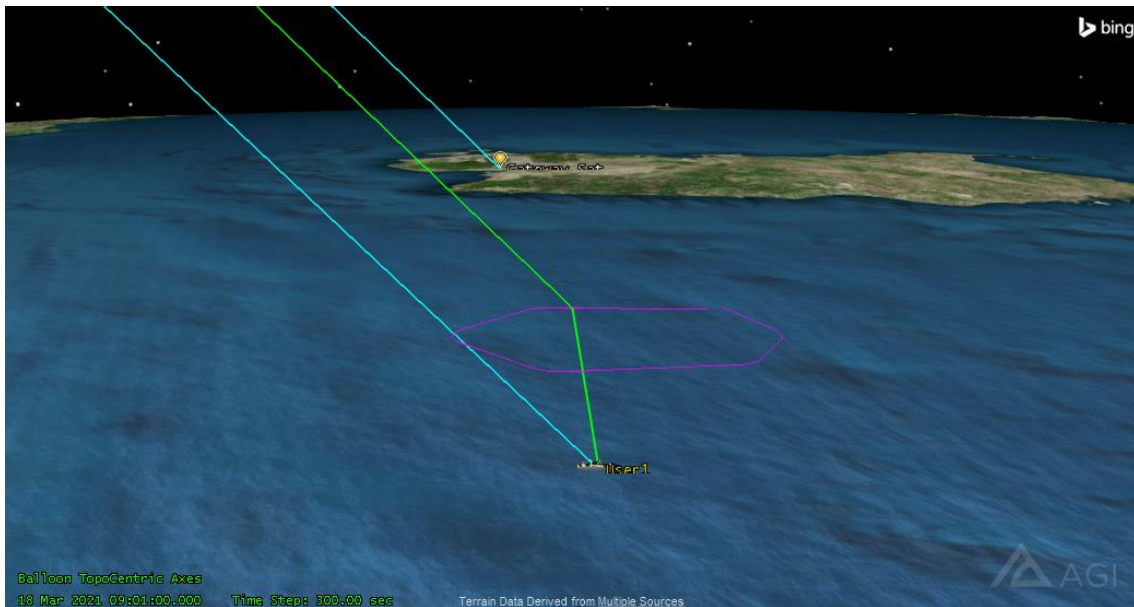


Figure 13 STK model: in cyan the satellite communication link, in purple the HAPS trajectory, in green the recovery link. Ship not in scale.

### 2.3.2 Link budget

As could be deduced, the weak link in the chain is the user to satellite uplink channel. This is due to the two factors:

- the constraints imposed on the UE that is designed to avoid the absorption of excessive power and to be compact, limiting the antenna size
- the RTN uplink frequency (29618,75 MHz) is heavily affected by rain attenuation

In Figure 14 are shown the effects of rain losses together with clouds and fog losses calculated as per ITU-R P840-6, with a cloud layer thickness of 0.3 km and a cloud ceiling placed at 4km. It is shown that rain and cloud losses can range from 5 dB up to 16 dB of loss and that can reduce the quality of the signal drastically.

In fact, while the FWD uplink channel, even suffering heavy attenuation, can still be closed thanks to the high gain antennas and to the - to a certain extent - not limited Tx power of the Gateway, the RTN uplink channel suffers much more rain and cloud attenuation and can potentially lose connectivity.

The UE can instead transmit to the HAPS, reducing de facto the link ranges from 35 786 km to less than 150 km, this will allow a grater margin to close the link with bad weather conditions. The HAPS will then route back the signal to the satellite with less power, bypassing the cloud layer.

In this scenario the HAPS is assumed to be equipped with a 60 cm parabolic both to receive from the user and to transmit to the satellite, and a transmitting power of 13 dBw (around 20 W).

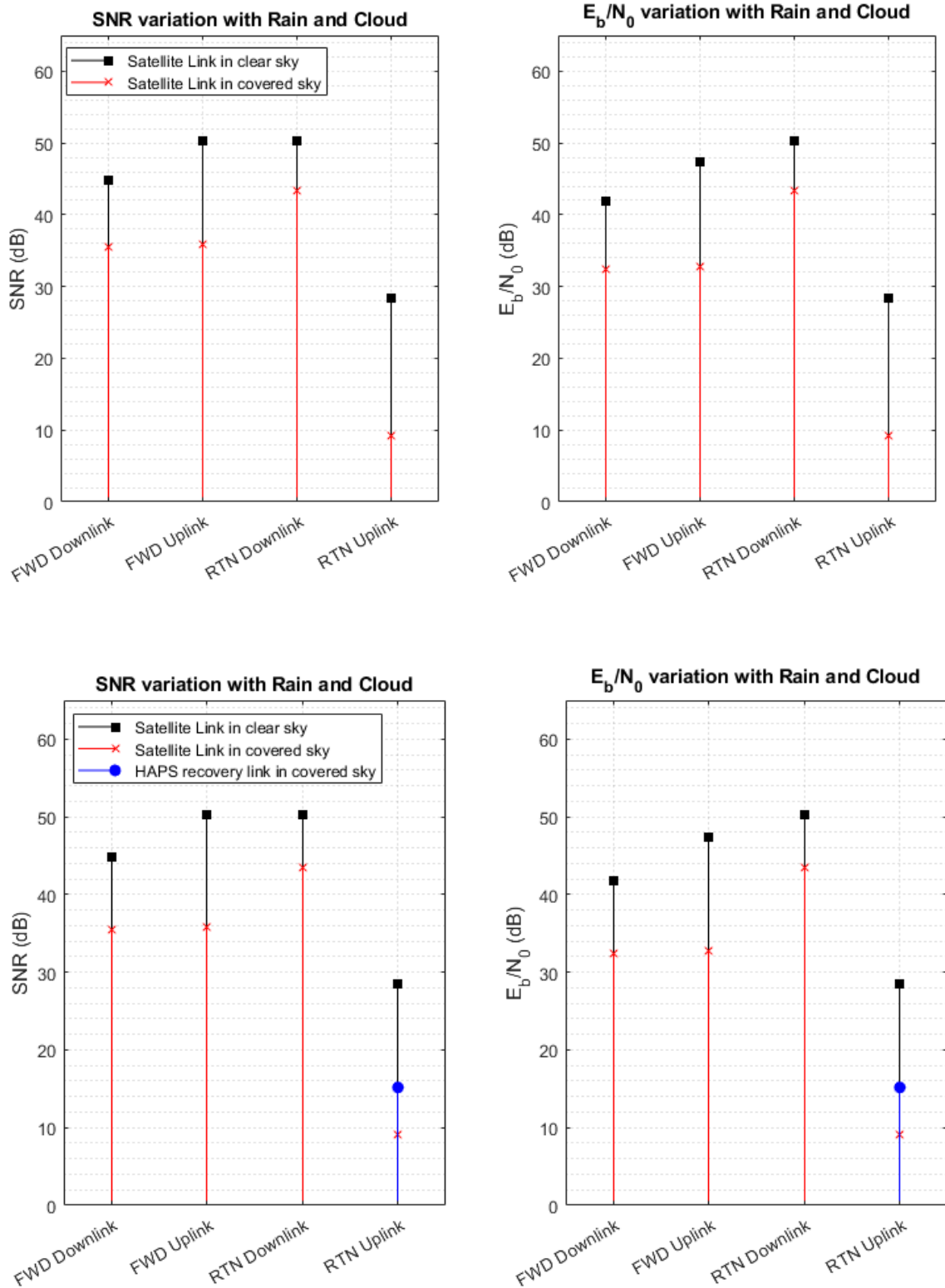


Figure 14 Effect of rain and cloud fade on GEO Ka communication link

### 2.3.3 Performances of the link

Tooway uses 16 APSK modulation to deliver internet at a maximum of 18 Mbps in downlink and 6 Mbps in uplink to a user in a spot beam (skylogic, 2012). However, for the intents of this thesis it will be assumed that QAM modulation is used.

The SNR in downlink is enough to allow the usage of 16 modulation APSK (16 QAM in out approximation) , while the link provided by the HAPS provides an uplink channel with around 15 dB of SNR, that is not enough to support the 16-QAM but is a good SNR for QPSK modulation (Figure 15).

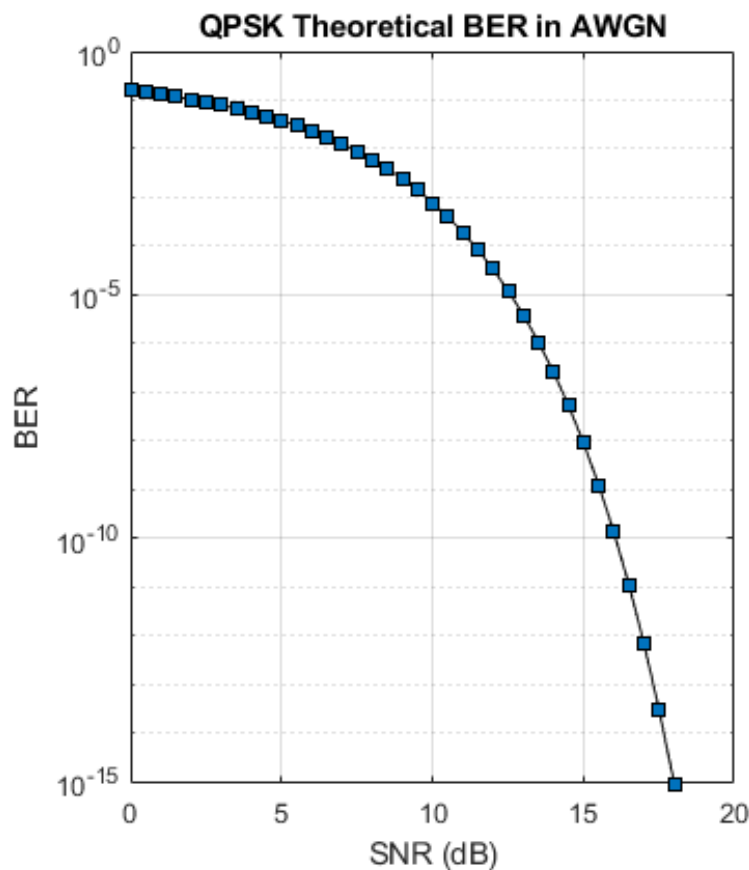


Figure 15 BER vs SNR for QPSK modulation

Since the bandwidth assigned to this service is 237.5 MHz, from this it can be computed how many users can be served by a single spot beam.

Considering that Tooway allows different service packages, ranging from 2 Mbps in downlink and 1 Mbps in uplink to 18 Mbps in downlink and 6 Mbps in uplink, an average data rate for each user can be reasonably estimated to be 12 Mbps in downlink and 4 Mbps in uplink. From that the number of users can be computed as:

$$\text{Number of users} = \text{Channel Throughput} / \text{Data Rate per user}$$

Again, as explained in 2.2.3, the Throughput can be computed as:

$$\text{Channel Throughput} = BW \times \text{Channel Utilization} \times \text{Spectral Efficiency}$$

with  $BW = 237.5 \text{ Mhz}$ ,  $\text{Spectral Efficiency} = N \times \text{FEC}$ ,  $N = 4$  for 16-QAM and  $N = 2$  for QPSK, and  $\text{Channel Utilization} = 1$

<i>Downlink 16-QAM</i>			<i>Uplink QPSK</i>		
<b>FEC</b>	<b>Channel Throughput</b>	<b>User Served</b>	<b>FEC</b>	<b>Channel Throughput</b>	<b>User Served</b>
1/2	475.0 Mbps	39	1/2	237.5 Mbps	59
3/4	712.5 Mbps	59	3/4	356.3 Mbps	89
7/8	831.3 Mbps	69	7/8	415.6 Mbps	103

**Table 9** Number of users served by a beam of a GEO satellite operating in Ka band

### 3 Advanced Payload Functional Design and Physical Baseline

The link side of this argument has been covered so far, the next step in designing a telecommunication payload for a light stratospheric platform is to outline a feasible functional and physical architecture that could satisfy the specifications. In these early stages of the project, requirements are not yet defined, some key drivers, however, are clear as the mission is well known.

#### 3.1 Key drivers

The main key drivers that will lead the design of the payload are established to be:

- Flexibility: it shall be possible to re-configure the payload RF parameters in flight
- Lightweight: the payload shall have a mass of less than 2 kg for a simple prototype that could be built and launched for initial testing
- Low power consumption: the payload will be powered by a battery rechargeable by photovoltaic cells, therefore the power shall be as low as the performances allow

#### 3.2 Elements of a telecommunication payload

A telecommunication payload usually corresponds to a wireless device that can receive and transmit information, hence, a transceiver. An RF transceiver is composed, at its essential level, in a transmitting line, a receiving line, a baseband processor and radiating elements to radiate the power over the air.

Transceivers are determined by how access to the Rx and Tx communication channels is managed. This may be half-duplex or full-duplex communication. Dedicated Rx or Tx devices are defined as operating in simplex mode. Full-duplex (FDX) transceivers can transmit and receive simultaneously using a diplexer or duplexer. Half-duplex transceivers (HDX) can receive or transmit but not both at the same time.

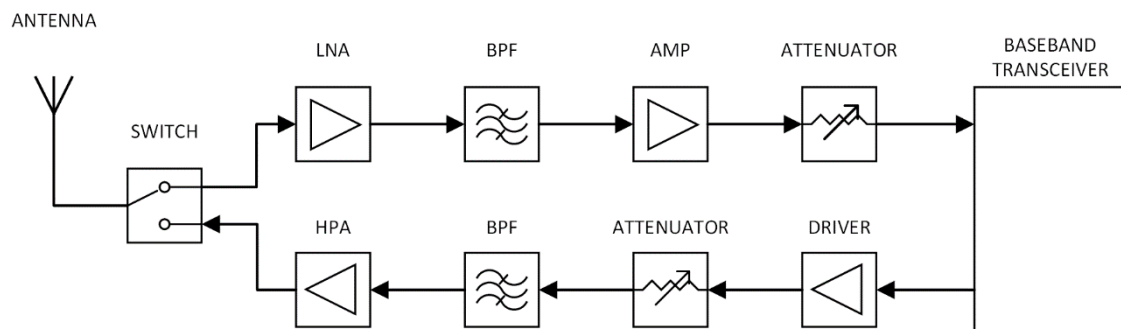


Figure 16 Example of a basic TDD RF transceiver configuration

Two type of baseband transceiver exist:

- Analogue transceivers: traditional type of transceivers, they use frequency modulation to send and receive information. Although this method limits the complexity of the data

that can be broadcast, analogue transceivers have the advantage of being highly reliable, therefore they are used in many emergency communication systems. The architecture they are based on is, generally, single purpose, for this reason they can also be cheaper than digital transceivers.

- Digital transceivers: they send and receive binary data over radio waves. This allows more types of data to be broadcast, including video and encrypted communication. Digital transmissions are much more general purpose and flexible than their analogue counterparts.

Other than the baseband transceiver, a RF layer is needed to provide the transceiver the correct quality of the signal to decode and transmit the information.

The RF layer can be split into three main parts:

- Radiating elements
- Receiver
- Transmitter

### **3.2.1 Radiating elements**

The radiating elements, commonly known as antennas, convert the oscillating voltage from a transmitter into a radio signal when used for transmission and capture radio signals out of the air translating into voltage while receiving.

Due to reciprocity, the same antenna can work both while transmitting and receiving, but to use it for simultaneous operations, different polarization and/or frequencies shall be used.

Efficiency, directivity, and gain are the key parameter that define the antenna performances:

- Efficiency is defined as the ratio of the radiated power to the input power of the antenna:  $\epsilon_R = P_{rad}/P_{in}$ .
- Directivity is the measure of the concentration of an antenna's radiation pattern in a particular direction. The higher the directivity, the more concentrated or focussed is the beam radiated by an antenna.
- Gain is the ratio of the power produced by the antenna from a far-field source on the antenna's beam axis to the power produced by a perfect isotropic antenna.

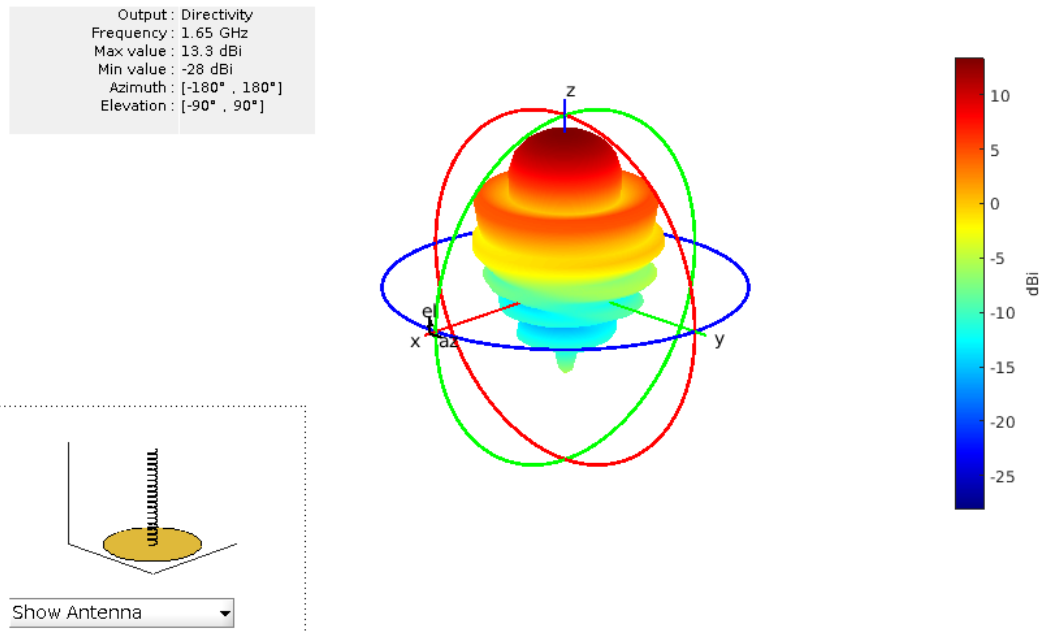


**Figure 17** Example of 3D directivity radiation pattern of a helical antenna at the centre frequency of 1.65 GHz

### 3.2.2 Receiver

The main functions of the receiver are to increase the SNR of the received signals, reject interference and noise and convert the received signal to baseband for demodulation. Usually can be reduced to a simplified model as in Figure 18.

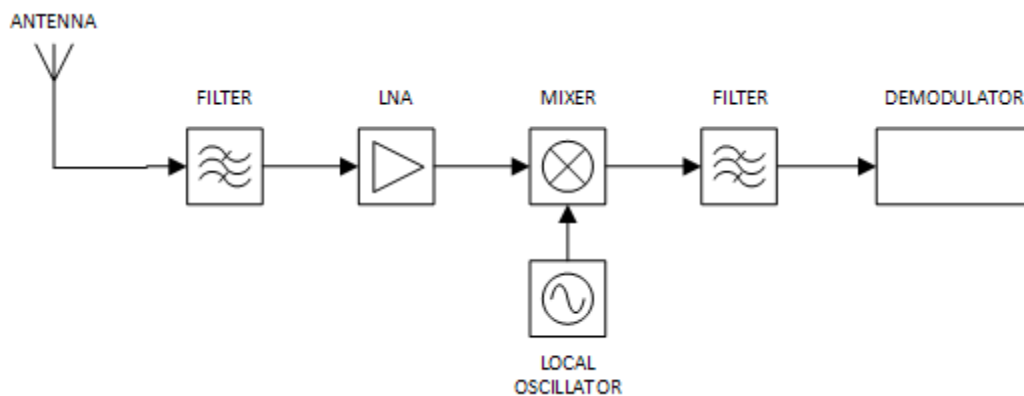


**Figure 18** Simplified receiver diagram

The ability to receive a good quality signal is highly affected by the antenna gain but, the noise temperature must also be included to account for the noise power that impacts on the performances of the receive line. Therefore  $G/T$  is the main parameter to consider when evaluating the quality of the received signal over a given location in the coverage of the HAPS.

$$G/T_{[dB/K]} = G_{antenna}[dBi] - T_{payload}[dBK]$$

where

$G_{antenna}$  is the receive antenna Gain

$T_{payload}$  is the Equivalent Noise Temperature of the Payload System

And

$$T_{payload} = 10\text{Log}(T_{antenna[K]} + T_{receiver[K]})$$

The Antenna noise temperature comes mainly by the natural radiation of the earth captured by the receive antenna while the electrical components in the equipment are the cause of the Receiver noise temperature and it can be reduced by cooling.

Each equipment in the receiver introduces thermal noise, at essential level, the noise is caused by the thermal agitation of the electrons in a conductor:

Absolute Noise Power in Watts:  $N_{[W]} = k_{[J/K]}T_{e[K]}B_{[Hz]}$

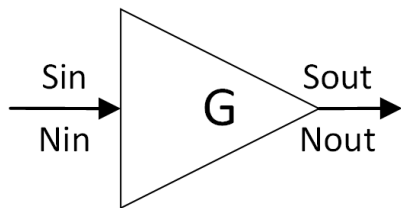
Noise Power Density in Watts/Hz:  $N_{[W/Hz]} = k_{[J/K]}T_{e[K]}$

Noise Power Density in dBW/Hz:  $N_{[dBW/Hz]} = -228.6 + T_{e[dBK]}$

where  $k$  is the Boltzmann's Constant =  $1.38 \times 10^{-23} \text{ J/K} = -228.6\text{dB}$ ;  $T_e$  is the Effective Noise Temperature in Kelvin and  $B$  is the Bandwidth in Hz.

The Effective Noise Temperature, however, often cannot be directly measured, therefore the Noise Factor  $F$  (or Noise Figure  $NF$  when expressed in decBels) is used and it is the main parameter to evaluate the quality of an LNA.

The Noise Factor is defined as the ratio of the signal-to-noise power ratio at the input to the signal-to-noise power ratio at the output (Keysight Technologies, 2010):



$$F = \frac{SNR_{in}}{SNR_{out}}$$

$$NF = SNR_{in[dB]} - SNR_{out[dB]}$$

For cascaded devices, as in the case of the payload receiver, the Friis's formula can be applied:

$$F_{receiver} = F_1 + \frac{F_2 - 1}{G_1} + \frac{F_3 - 1}{G_1 G_2} + \frac{F_4 - 1}{G_1 G_2 G_3} + \dots + \frac{F_n - 1}{G_1 G_2 \dots G_{n-1}}$$

Each term contributes to the overall receiver noise temperature, but, is notable that, before the LNA, there is no gain, only losses ( $L = 1/G$ ), therefore, equipment up to and including the LNA have the highest contribution to the Receiver Noise temperature.

Filtering stages are also needed both to avoid G/T degradation due to Noise Feedback from the HPA and to filter out the unwanted signals received by the antenna or created by active equipment (Amplifiers, mixers etc.). Furthermore, HAPS are subject to interference created by other infrastructures operating in the same or neighbouring frequencies as they have no priority

over Fixed Services. HAPS, in fact, cannot claim protection from other fixed service systems or co-primary services

### 3.2.3 Transmitter

A transmitter carries out the functions of modulating the signal, shifting its frequency and, ultimately, amplifying the signal providing high power to the antenna, Figure 19.

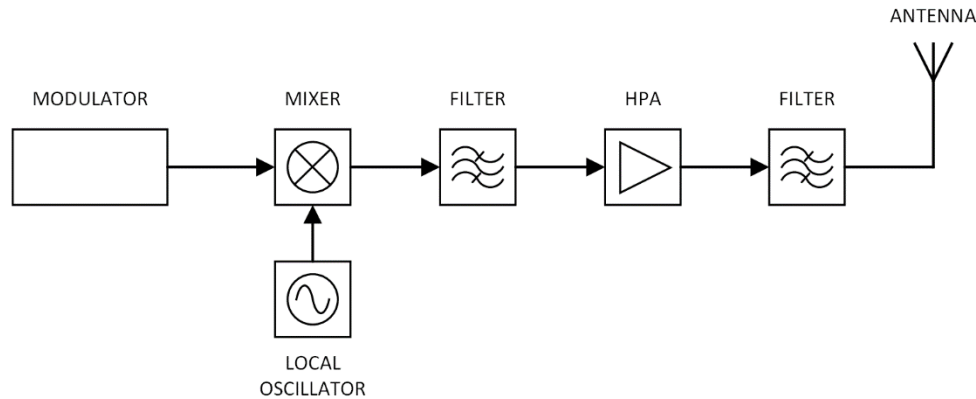


**Figure 19 Simplified transmitter diagram**

The main contributors to the transmitter performances is the High-Power Amplifier together with the Tx antenna:

$$EIRP_{[dBw]} = G_{TxAntenna[dBi]} + P_{Tx[dBW]}$$

where

$G_{TxAntenna}$  is the isotropic gain of the transmit antenna

$P_{Tx}$  is the transmitter output power calculated from  $P_{HPA} - L_{output}$

$L_{output}$  is the loss of the output section (from the HPA until the antenna feed)

EIRP is usually defined at saturation (the point of maximum output power of the HPA), but typically HPAs have a non-linear gain characteristic, therefore they are operated at Back-Off (BO). Back off can be specified from the input power to saturate the HPA: Input Back-Off (IBO), or from the saturated output power: Output Back-Off (OBO), see Figure 20.

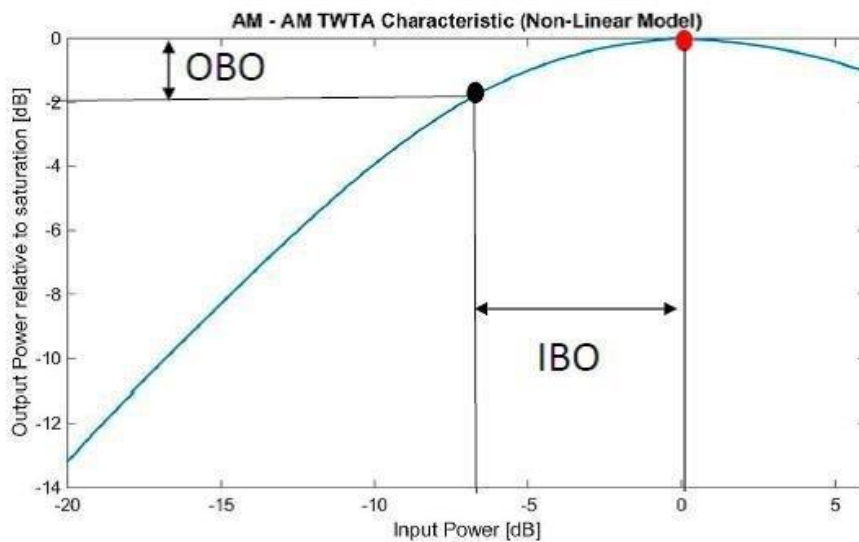


**Figure 20 HPA Pin/Pout transfer curve and Back-off operation**

Operating the HPA at saturation can distort the signal being amplified generating intermodulation products or disturbing amplitude and phase linearity of the signal, therefore HPAs should be operated at back-off. Other techniques to operate closer to the saturation point include the use of a pre-distortion system before the HPA or the implementation of a compensating equalizer at the receiver level. More complex techniques can also be investigated.

Is, therefore, evident that filters are needed in the output section to cut out the 2<sup>nd</sup> and 3<sup>rd</sup> order harmonics and to reject the unwanted signals and noise generated by the HPA that will otherwise induce noise feedback in the input section of the payload and degrade its G/T.

Given the high power in the output section, isolators are used to prevent the highly energetic waves to flow backwards damaging the hardware

At last, after the filtering stages Passive Intermodulation Products (PIM) can be created by discontinuities, joints, defects, cracks, nonlinear materials and so on. If one of the unwanted signals created is then fed into the Rx section it could degrade the payload performances.

### **3.2.4 Software Defined Radios**

To cope with the flexibility driver given in this first stage of the project, where the operating frequency band is still unknown, the best option is to consider digital components, at least for the baseband processing layer, therefore, using Software Defined Radios is natural pick. In fact, trying to design an analogue payload when the service to provide is still undefined would be too complicated.

Furthermore, SDR will provide optimal room for experimentation and prototyping, especially during the first periods of testing.

An SDR is defined as a radio system in which some or all the functions of the physical layer are implemented in software using Digital Signal Processing (DSP) (Book by Dale S W Atkinson, 2015). The primary goal of SDR is, indeed, to replace as many analogue components and

hardwired digital devices. The incoming analogue signals are, therefore, converted to digital signals using an Analogue-to-Digital Converter (ADC), demodulated using software running on a superfast processing core then, the processed digital signal is converted to an analogue signal using a Digital-to-Analogue Converter (DAC) and transmitted again after modulation.

Many smartphones and connected devices now have different radios optimised for receiving various signals from different frequency bands. A common smartphone can communicate using WiFi (2.4 GHz), LTE (800 MHz), GSM (900 MHz), GPS (1.5 GHz), Bluetooth (2.4 GHz), NFC (13.56 MHz) and so on, with intention of expanding these capabilities to incorporate IoT, 5G and etc. The optimal solution here would be to utilize an SDR to receive all of these signals and implement all the receivers in software.

Essentially, SDR are composed by an RF section (antenna, amplifiers and filters) and a very high-speed ADC and DAC pair, interfaced with a powerful computing system that can sustain the sampling rate.

Recalling the Nyquist- Shannon theorem, for perfect reconstruction of the signal is guaranteed if the sample rate is greater than twice the signal bandwidth:

$$B < f_s/2$$

Therefore, the capabilities of an SDR (in terms of baseband spectrum in which it can operate) are dictated mainly by its sampling rate.

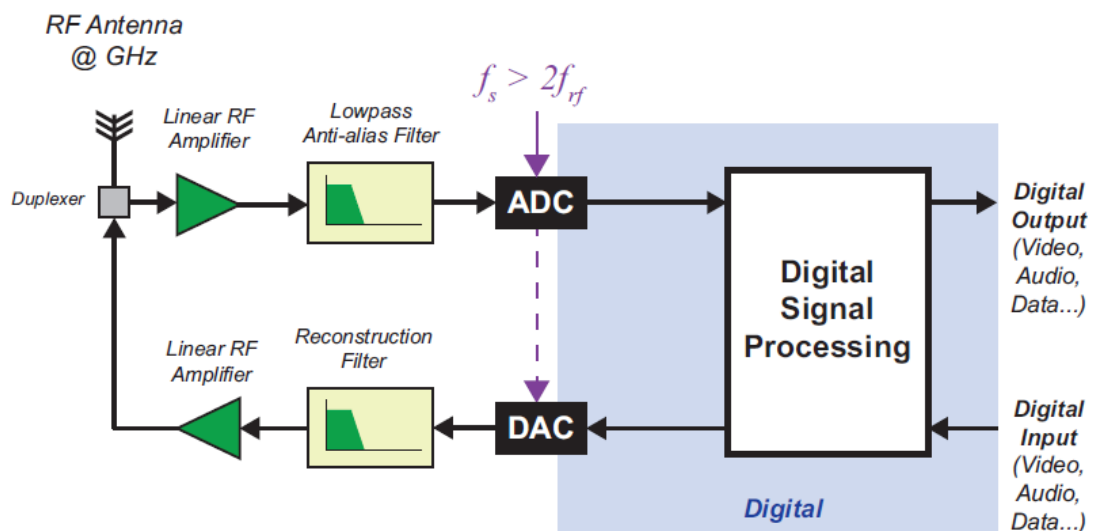


Figure 21 Components of a conceptual SDR. **INSERT SOURCE**

### 3.3 Functional Baseline

Architectures of various complexity were produced for Stratobotic, all of the designs are intended for FDM operations.

As explained in 293.2.4, the payload, at this stage, is based on SDRs, which will take away the need for mixers and oscillators when operating in the SDR frequency range, reducing overall

cost, mass and power required. As today, the average performances of a light SDR can allow to sample until 6 GHz, although SDRs that can operate until 73 GHz exist. (wikipedia, s.d.)

The bladeRF 2.0 SDR (nuand, s.d.), given its strong flexibility, portability and its extensive documentation, is an ideal candidate to begin the experimentation with: it has a mass of less than 400 g, it supports GNU Radio, is open source and it is supported by a wide community that provides source code for many applications.

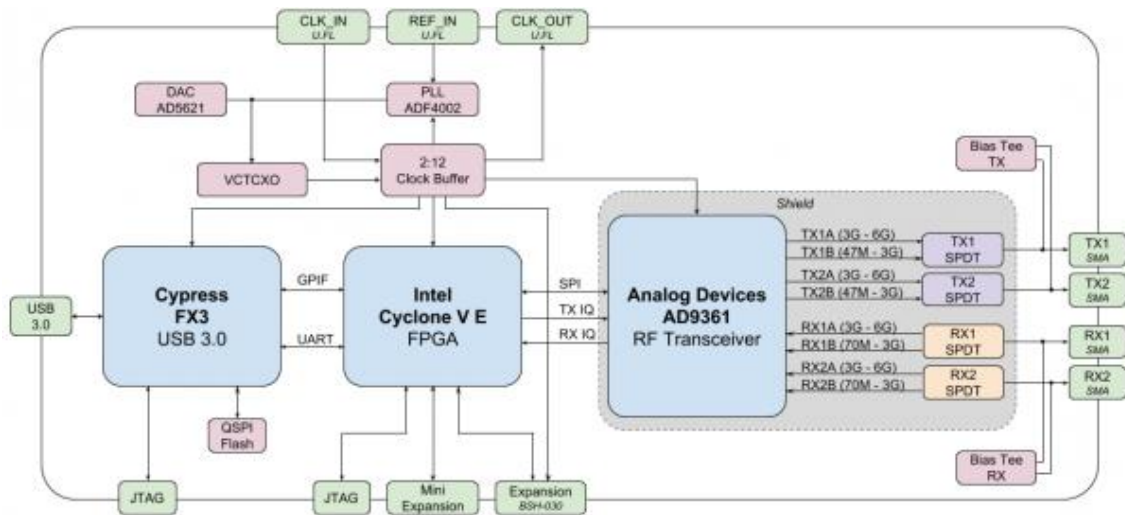


Figure 22 nuand bladeRF 2.0 microA9 block diagram

The receiver RF layer is composed as follows:

- Rx/Tx antenna: will be defined in detail in subsequent stages of the project, currently is assumed to be composed by a reflector and a feed
- Input filter: screens unwanted signals out such as transmission feedback and other interfering frequencies coming from terrestrial and/or space networks
- LNA/Limiting LNA: amplifies the signal without degrading the SNR. It can be, potentially, substituted with a limiter LNA to include overdrive protection and/or anti-jamming capabilities
- Selection switches and filters: can be included for service selectivity, they can be used when the number of services to carry onboard in a flight (i.e. LTE, 5G, GSM, WiFi etc.) is greater than the number of useable HPAs
- Bias-Tee LNA: provides a degree of freedom to further amplify the received signal controlling the gain via software.

In transmission:

- Bias-Tee Power Amplifier: provides a degree of freedom to amplify the transmitted signal via software to adapt the HPA input power to the operational point
- HPA: Amplifies the transmitting signal
- Circulator and terminator (isolator): allow the propagation of the signal only towards the Tx antenna, shielding the preceding equipment
- Output filter: removes harmonics and thermal noise produced by the HPA, prevent degradation of G/T due to Noise Feedback

The functional architecture of such payload is represented in Figure 23. It is a simple architecture to communicate in LOS with a user or a ground station (i.e. using the same reflector in Tx and Rx changing its polarisation), it can also be used for BLOS communication links in simplex mode.

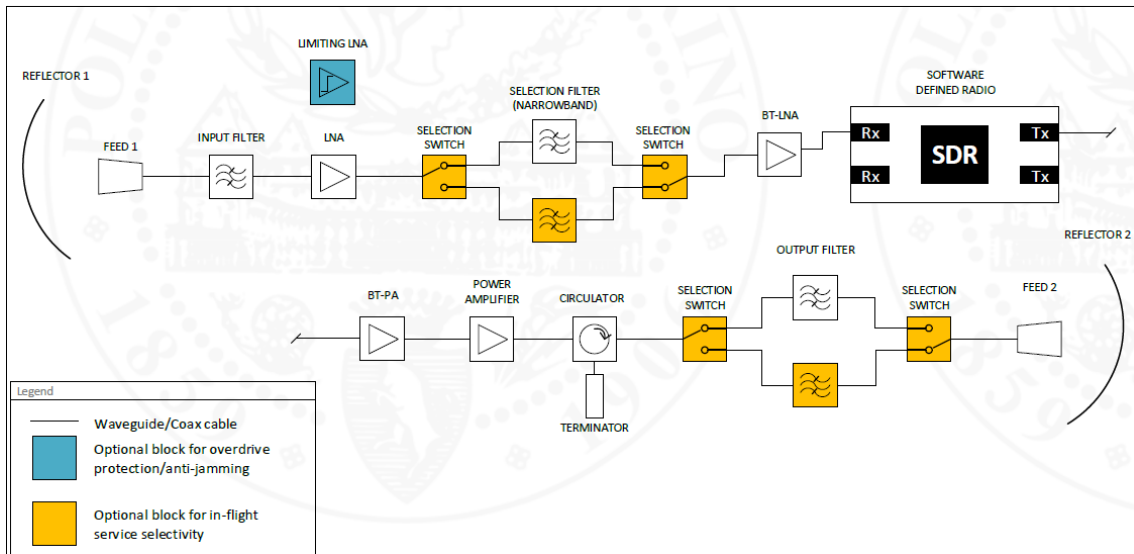


**Figure 23 Simple 1x1 payload architecture**

A more complete architecture that can achieve BLOS full duplex operations is shown in Figure 24. Such architecture is the most versatile and can allow implementation of 2x2 MIMO techniques. This can extend the capacity of the radio links exploiting multipath propagation, increasing the capabilities of such design for HAPS applications.

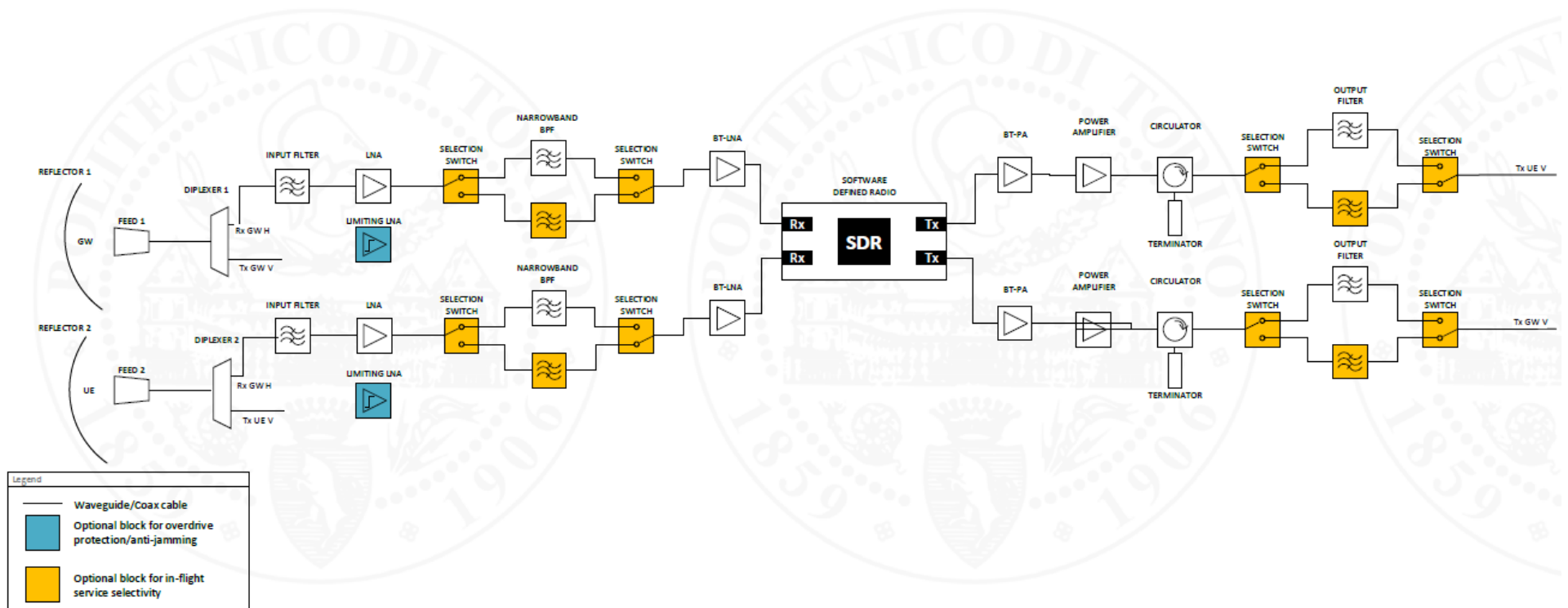


Figure 24 complete 2x2 payload architecture

To build preliminary budgets equipment from (pasternack, s.d.) have been used as reference.

		Architecture #1	Architecture #2	Architecture #3	Architecture #4
<b>Cost (EUR)</b>		<b>17,337 €</b>	<b>47,706 €</b>	<b>24,228 €</b>	<b>55,919 €</b>
<b>Mass (g)</b>		<b>1815.7</b>	<b>2093.2</b>	<b>2279.4</b>	<b>2502.6</b>
<b>Nominal Power (W)</b>	<b>Tx + Rx</b>	<b>11.4</b>	<b>17.2</b>	<b>18.3</b>	<b>29.8</b>
	<b>Tx</b>	<b>8.7</b>	<b>9.7</b>	<b>14.9</b>	<b>14.9</b>
	<b>Rx</b>	<b>6.2</b>	<b>12.0</b>	<b>7.9</b>	<b>19.4</b>

Table 10 Payload budgets for different architectures

### 3.4 Simulation

To assess the performances of the RF receiver front-end a Simulink model has been created. The transmitted data, modulated with either M-QAM or QPSK in this case, can be affected by distortion that simulate the effects of wireless transmission such as addition of Additive White Gaussian Noise (AWGN) or carrier frequency and phase degradation, or any other effect induced by equipment such as filters, amplifiers and so on. To cope with these impairments, this model provides a reference design of a practical digital receiver, that can be expanded and used in the future to analyse the performances of the payload with different configuration before the testing phase.

For this model, MATLAB/Simulink blocks from Communications Toolbox and DSP System Toolbox™ are used to perform baseband signal processing and RF Toolbox to build the RF front end; the RF Toolbox provides functions, objects, and tools for designing, modelling, analysing, and visualizing networks of RF components and is particularly useful to model the behaviour of real hardware.

The model is divided into three main subsystems as per Figure 25:

- Source + Channel
- Receiver RF Front End
- ADC and Digital Receiver

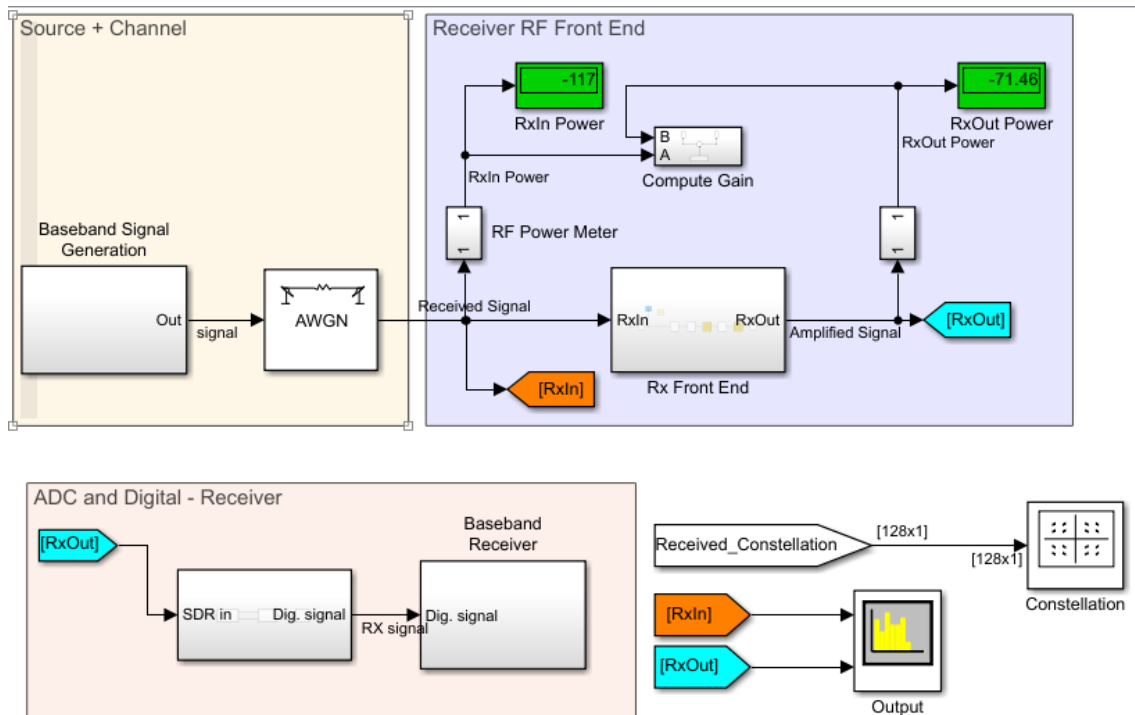


Figure 25 Digital Receiver model in Simulink

### 3.4.1 Source and Channel

Source + Channel generates the baseband signal as a random uniformly distributed bit stream, then modulates it using rectangular QAM method and raised cosine filtering to minimise intersymbol interference (Figure 26). The raw bits generated are passed to the receiver to be compared with the received bits in order to compute the BER.

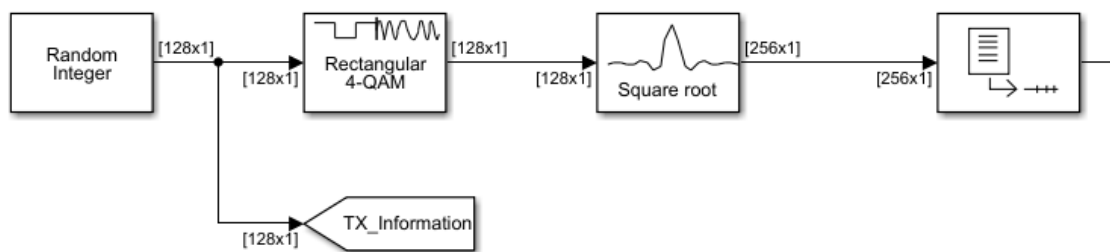


Figure 26 Baseband Signal Generator in the Simulink model

An AWGN block is added to model impairment due to linear addition of white noise with constant spectral density calculated with the  $SNR$  and the Input Signal Power.

### 3.4.2 Receiver RF Front End

The Receiver RF Front End consists of the RF layer and power meters to measure the overall Gain across the receiver. The RF layer has been set to match the design presented in Figure 23

and equipment data has been retrieved from datasheet of components suitable for the application of interest.

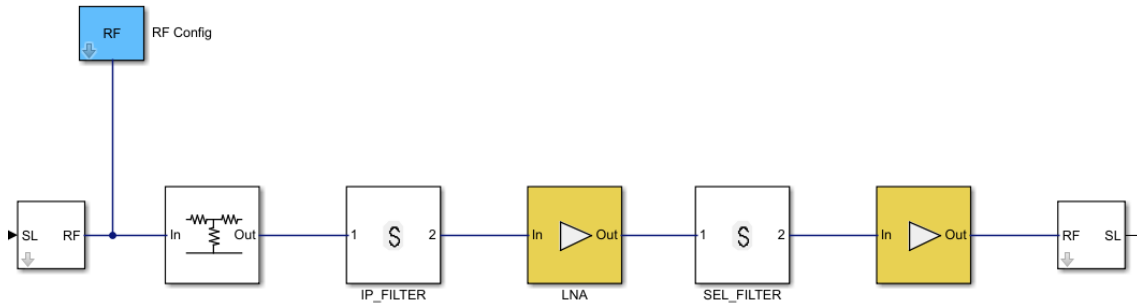


**Figure 27 Simulink Receiver RF Front End**

The first and the last blocks convert Simulink signal to RF Blockset Circuit Envelope voltage and vice versa.

The RF Config block (in blue) is used to select the RF simulation settings such as the Carrier Frequency and the harmonic order.

To simulate the behaviour of cables and waveguides an ideal resistive load is used to simulate its loss. Ideally, when a more detailed design will be available, any ancillary equipment, such as cables, connectors, attenuators and similar, could be modelled as pure loads as their response is generally purely resistive.

To model the filters, real data of commonly used ceramic filters have been used: the data have been retrieved in the form of scattering parameters from a manufacturer website ([www.minicircuits.com](http://www.minicircuits.com), s.d.). S-PARAMETERS allow the highest fidelity in the description of the electrical behaviour of the RF path, therefore, they should be used whenever it is possible. In Figure 28 is shown the input filter response.

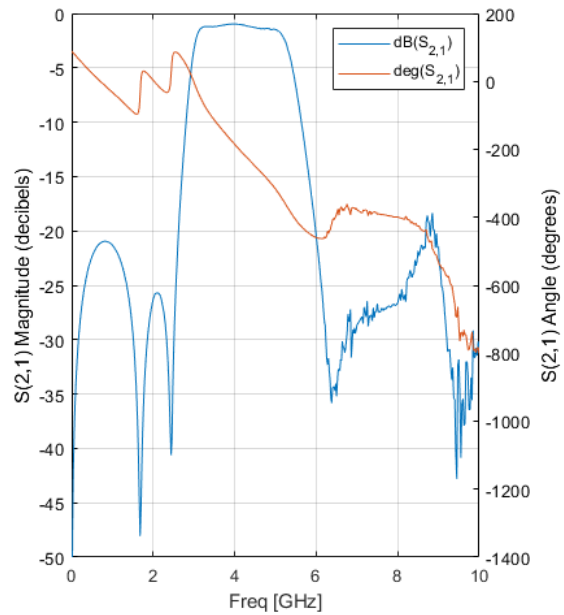


**Figure 28 Input Filter S21 parameter**

To model the amplifiers, the Simulink RF Toolbox provides a default block that can easily represent the linear and non-linear behaviour of the component. For the LNA the following parameters have been used:

$$G = 40 \text{ dB}, IP3 = 25 \text{ dBm},$$

$$P1dB = 14 \text{ dBm}$$

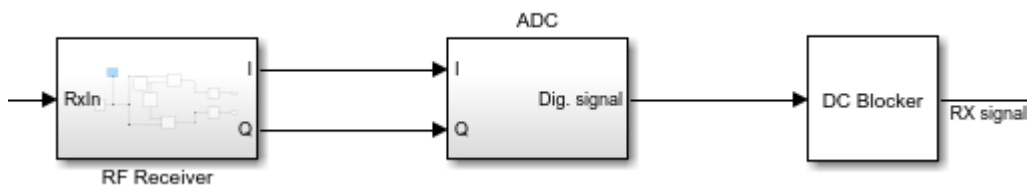
$$OPS = Inf$$

$$NF = 0.9 \text{ dB}$$

data retrieved from (pasternack, s.d.)

### 3.4.3 ADC and Digital Receiver

The ADC and Digital Receiver consists of a RF receiver, and ADC and a Baseband Receiver. Is a simplified model of the bladeRF 2.0 (Figure 22) therefore its specification have been taken as reference: ADC/DAC Resolution of 12 bits and ADC/DAC Sample Rate.



The last subsystem, that is the Baseband Receiver, contains all the demodulation chain to interpret the symbols and it calculates the BER (or SER, Signal Error Rate, as in Figure 29) and shows the received constellation.

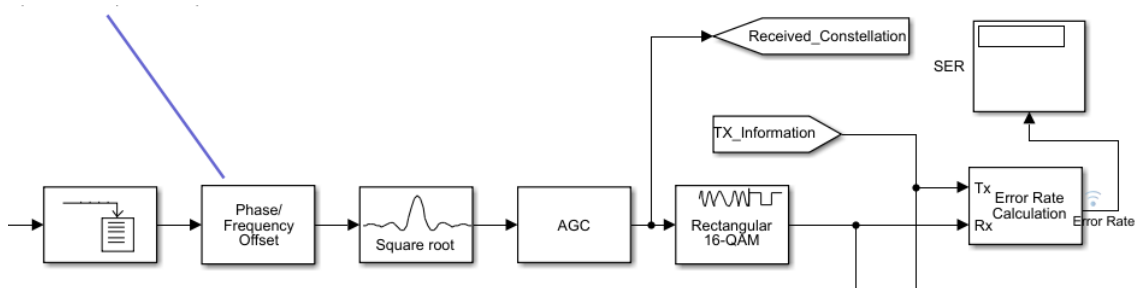


Figure 29 Simulink Baseband Demodulator

The BER is computed as:

$$BER = \text{Incorrect Received Bits} / \text{Total Transmitted Bits}$$

### 3.4.4 Output and Results

Running the simulation (with the Accelerator mode enabled to reduce the computation time), it is possible to see the nearly real time spectrum of the channel under analysis (Figure 30) that shows:

- the received signal (yellow spectrum) after the addition of white noise at the selected input power and SNR, in this case respectively  $-114\text{ dBm}$  and  $20\text{ dB}$
- the amplified signal after passing through the RF layer of the receiver (blue spectrum). This is particularly useful as it could show how different equipment affect the received signal quality and optimise performances. This could also be used to assess if any nonconformity in the hardware acts on the gain versus frequency response of the payload and to what extent and/or in band spurious signals.

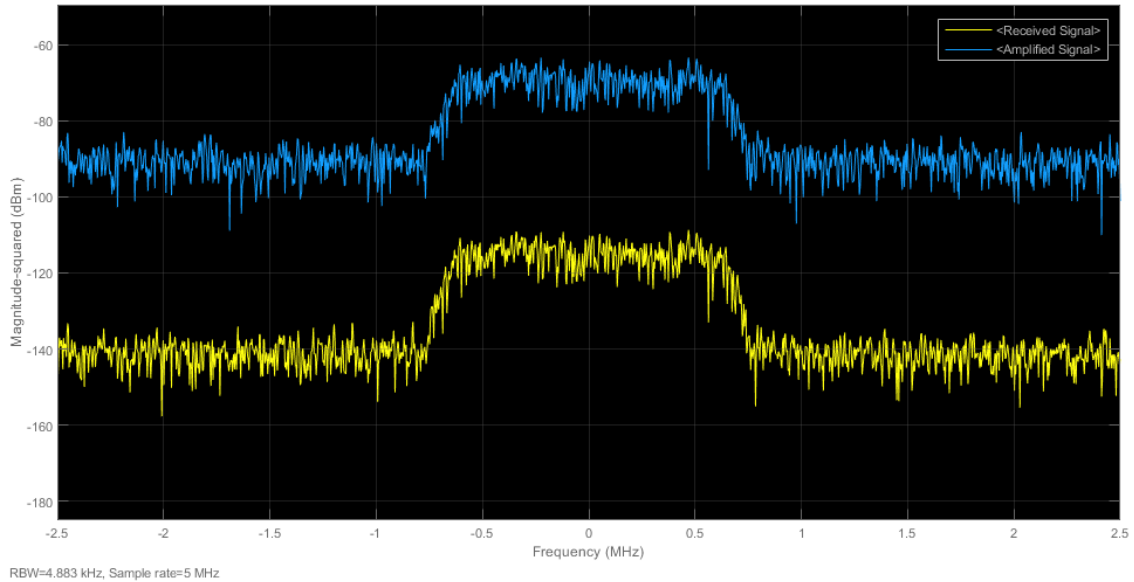


**Figure 30 Output spectrum of the simulation**

Simulink allows also to create the signal constellation. The constellation is a diagram on the Gauss plane that represents all the possible states of the carrier(s) and, therefore, all the possible position that the reference vector can assume (red marks). Each vector is mapped to a symbol, a 16-QAM has 16 symbols hence 16 marks on the diagram.

On top of that, the detected symbols decoded by the receiver are shown (yellow dots), and it is possible to understand how well each symbol is received computing the Error Vector Magnitude (EVM). The EVM is a measure of the quality of the modulation and can be used to determine the signal reliability together with the BER.

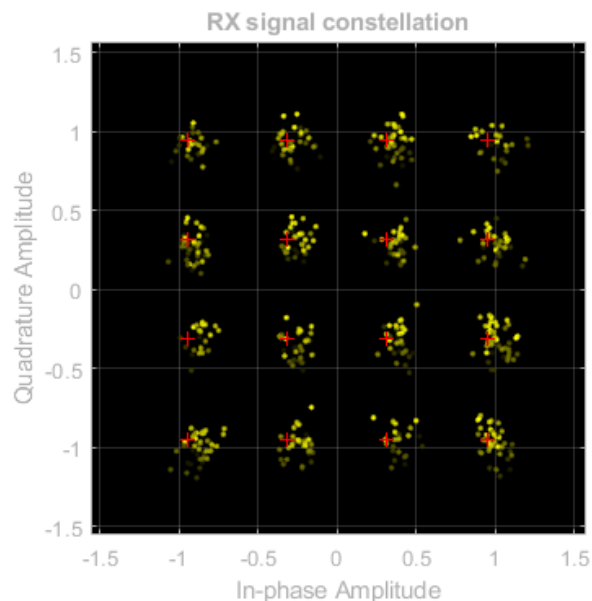


**Figure 31 Rx signal 16-QAM constellation at 20dB SNR**

Furthermore, as different impairments have different effect on the constellation, this diagram is also useful to spot common radio methods of signal degradation such as amplifiers nonlinearity, I/Q impairments, phase noise, etc.

To validate the model some analyses have been run and checked against the theoretical SNR required for different QAM (see Figure 11 for reference).

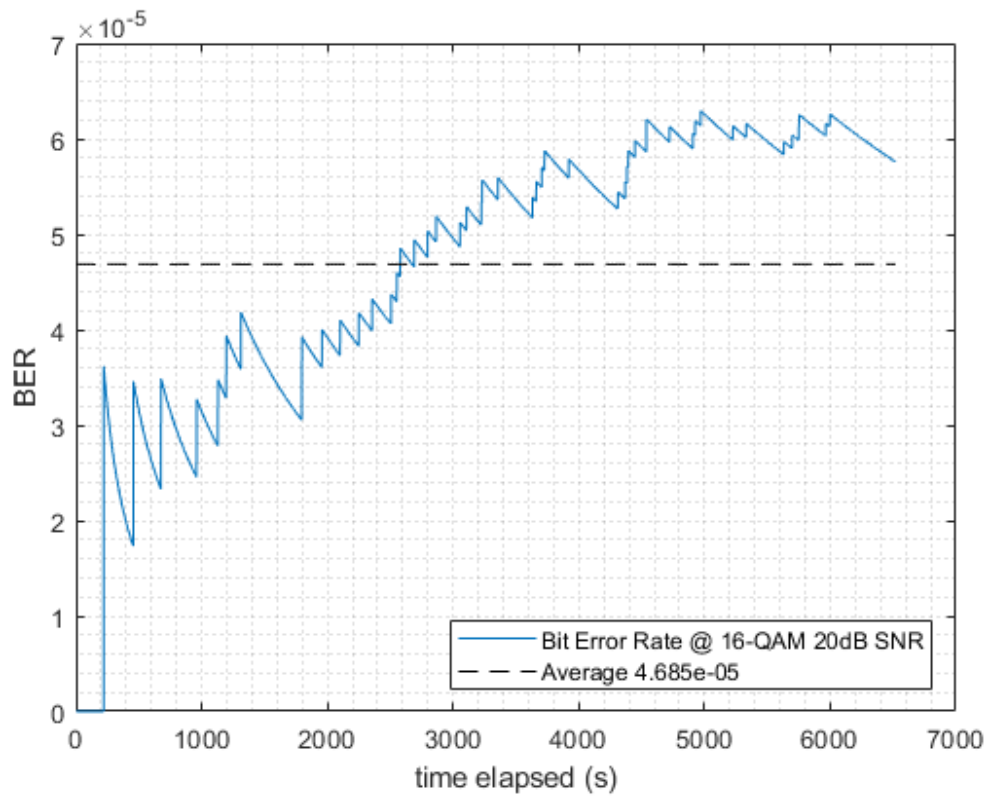


Figure 32 Simulation of the Bit Error Rate for a 16-QAM

## 4 Prototyping

The early stages of prototyping include a phase of study and test of commercial transceivers already on the market. This allow to set standards of performances and build a practical background based on already proven hardware to validate the theoretical and engineering models.

The Microhard pMDDL5824 was selected by Stratobotic for this purpose.

### 4.1 Microhard pMDDL5824

This commercial transceiver is a dual band digital modem that supports 2X2 MIMO. It operates in the Wi-Fi bands (2.4 – 5.8 GHz) allowing bandwidth selection from 1 to 8 MHz.

The main applications of this device include High-Speed backbone, ethernet wireless extension, UAV/UAS, multicast video, remote telemetry etc.

The transmission power can range from 20 dBm to 30 dBm and its maximum performances allow a maximum data rate of *27.8 Mbps*, obtained with (2X2) MIMO ON, 8 MHz bandwidth with 64 QAM modulation with 5/6 FEC:

MIMO (2X2) ON			
Modulation	IPerf Throughput (Mbps)	Throughput @ Sensitivity (dBm)	Maximum Total Tx Power (dBm) +/- 1dB
<i>8 MHz Channel Bandwidth</i>			
QPSK_1/2	5.9	-98	30 dBm
QPSK_3/4	8.8	-96	30 dBm
16QAM_1/2	11.6	-92	30 dBm
16QAM_3/4	17.1	-90	30 dBm
64QAM_2/3	22.8	-85	30 dBm
64QAM_3/4	25.5	-83.5	30 dBm
64QAM_5/6	27.8	-81	30 dBm

**Table 11 Microhard pMDDL5824 performance specification @ maximum bandwidth and MIMO ON**

The receiver sensitivity varies upon the channel bandwidth, in fact, a larger channel can deliver more throughput at the expense of sensitivity, while selecting a smaller channel will increase the sensitivity (therefore the channel robustness), at the cost of throughput.

The pMDDL5824 can be operated in different modes that are:

- Master: is the communication hub that can start a wireless connection with one or more devices (Slaves)
- Slave: can communicate with only one other device (Master)
- Repeater: provides wireless connection to a Master/Repeater and many remotes
- Mesh: if all the units are configured as Mesh nodes, the data will find a path through the mesh until it reaches its end point. It is used to increase reliability adding redundancy and raising the possible routes, however the overall throughput will decrease

For the purposes of this work, only the Master/Slave operating mode is considered as it allows to provide a Point-to-Point communication link (i.e. balloon – ground station) or a Point-to-Multipoint communication link (e.g. ground station – balloon – user, balloon – multiple users, ground station – balloon – balloon and so on).

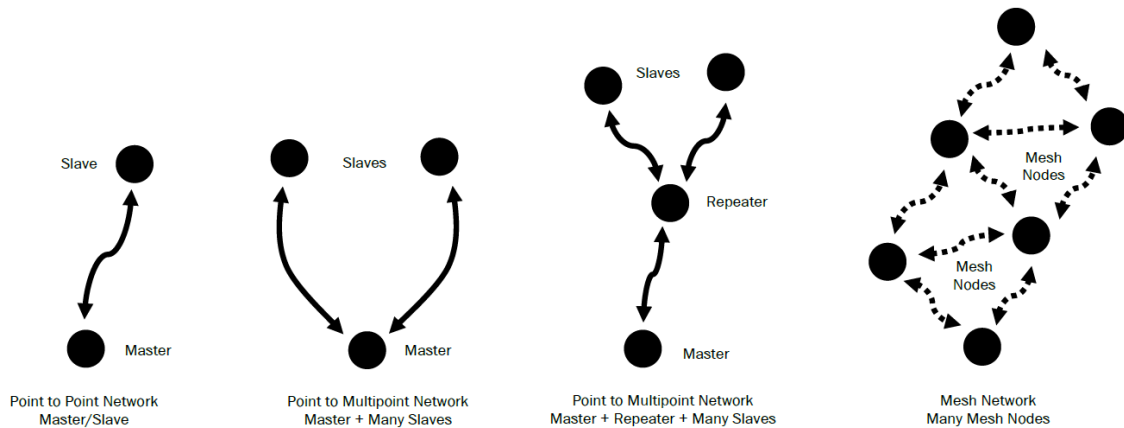


Figure 33 pMDDL5824 operating modes

Accessing the network and the RF proprieties of the device is a straightforward process that consists of connecting a computer to the pMDDL5824 via an ethernet cable and entering its IP address in a web browser address bar. This allows to setup and configure LAN, WAN, Wireless, DHCP and any other feature by web user interface. However, this is not ideal, especially for configuring the transceiver in flight, as the web browser will not be accessible.

Therefore, a python code to access to the router configuration has been written. The code uses the Telnet protocol to communicate with the pMDDL5824.

```

Telnet 192.168.168.12
UserDevice login: admin
Password:

Entering character mode
Escape character is '^]'.

Command Line Interface
UserDevice> AT+MMSTATUS
General Status
MAC Address      : 00:0F:92:FC:05:72
Operation Mode   : Slave
Network ID       : pMDDL_TEST
Bandwidth        : 8 MHz
Frequency        : 5076 MHz
Tx Power         : 7 dBm
Encryption Type  : AES-128
Tx Antenna Chains : 1
Rx Antenna Chains : 1
Traffic Status
Receive Bytes    : 5,516MB
Receive Packets  : 33922
Transmit Bytes   : 4,593MB
Transmit Packets : 29578
Connection Info
MAC Address      : 00:0F:92:FC:05:7C
Tx Mod (MIMO)    : 64-QAM FEC 5/6 (Off)
Rx Mod (MIMO)    : 64-QAM FEC 5/6 (Off)
SNR (dB)         : 36
RSSI (dBm)       : -62 [-62] dBm
Noise Floor (dBm) : -98
OK
  
```

Figure 35 example of network status retrieving via Telnet

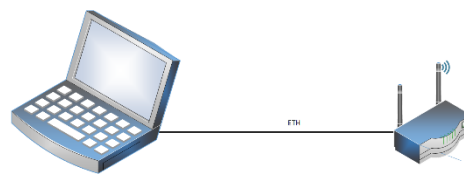


Figure 34 Setup to configure the Microhard transceiver via laptop

Telnet is an application protocol that allows to control devices such as routers, switches, hubs and gateways remotely using a bidirectional text-oriented connection over TCP/IP, this is especially useful both to telecommand (TC) the transceiver remotely from a ground station and to read the e status of the device to create a telemetry (TC).

As it uses TCP/IP, Telnet allows to communicate with any other transceiver in the network and it is supported by any OS. In short, is an easy and valuable tool to command and control the devices.

However, it should be used only during the prototyping phase. Telnet, in fact, does not encrypt

the data sent over the network, including the credentials used to access to the transceivers, exposing the connection to malicious intents.  
It should be considered, in the future, to operate the modems via Secure Shell (SSH).

```
import getpass
import time
import telnetlib
import re

HOST = "192.168.168.11"      #host IP address
input("Enter your remote account: ")
password = getpass.getpass("Password for " + user + ":")

#function to improve readability of output strings
def printTelnetOutput(tn, expected, tout):

tn = telnetlib.Telnet(HOST)      # create a telnet session with the
HOST                               # HOST
tn.read_until("login: ".encode()) # read till it finds the expected
login script
tn.write((user + "\n").encode())  # write the username to telnet
if password:
    tn.read_until("Password: ".encode())
    tn.write((password + "\n").encode())

time.sleep(2)

printTelnetOutput(tn, b"Command Line Interface", 2) # display
tn.write("AT+MWRADIO=1\n".encode())                # set the
radio on
printTelnetOutput(tn, b"OK", 2)                    # display
tn.write("AT+MWVMODE=0\n".encode())                # set
operating mode to master
printTelnetOutput(tn, b"OK", 2)                    # display
tn.write("AT+MWTXPOWER=7\n".encode())              # set power
level
printTelnetOutput(tn, b"OK", 2)                    # display
tn.write("AT+MWRBAND=0\n".encode())                # set
operating band
printTelnetOutput(tn, b"OK", 2)                    # display
tn.write("AT+MWBAND=3\n".encode())                # set
operating channel
printTelnetOutput(tn, b"OK", 2)                    # display

print("all done")
tn.close() #close the active telnet session
```

## 4.2 Preliminary configuration and testing

This section describes the activities carried out in Stratobotic's laboratory to prepare the flight prototype for its first demonstrations.

In the early phases of primary interest will be to assess the capabilities of the HAPS to communicate with a ground station and exchange data through a communication link.

The HAPS on board computer, at least at this stage, is a Raspberry Pi 4, a single board computer known for its low cost, modularity, and open design. Its OS is Raspbian, a Debian-based operating system that runs on a Linux Kernel. The Raspberry products benefit from a wide community that exchanges code and libraries to build and enhance projects.

The raspberry, in most of the cases, will be connected to a Master as it will be the hub of ground stations and users, while a laptop, representing a ground station in this case, will be connected to a Slave transceiver.

### 4.2.1 Telemetry, Telecommand and Payload data stream

The objective of this test consists in sending a request from a ground station (laptop) to retrieve the real time telemetry (in this case only IMU data) from the Raspberry.

The setup for this test is shown in Figure 36.

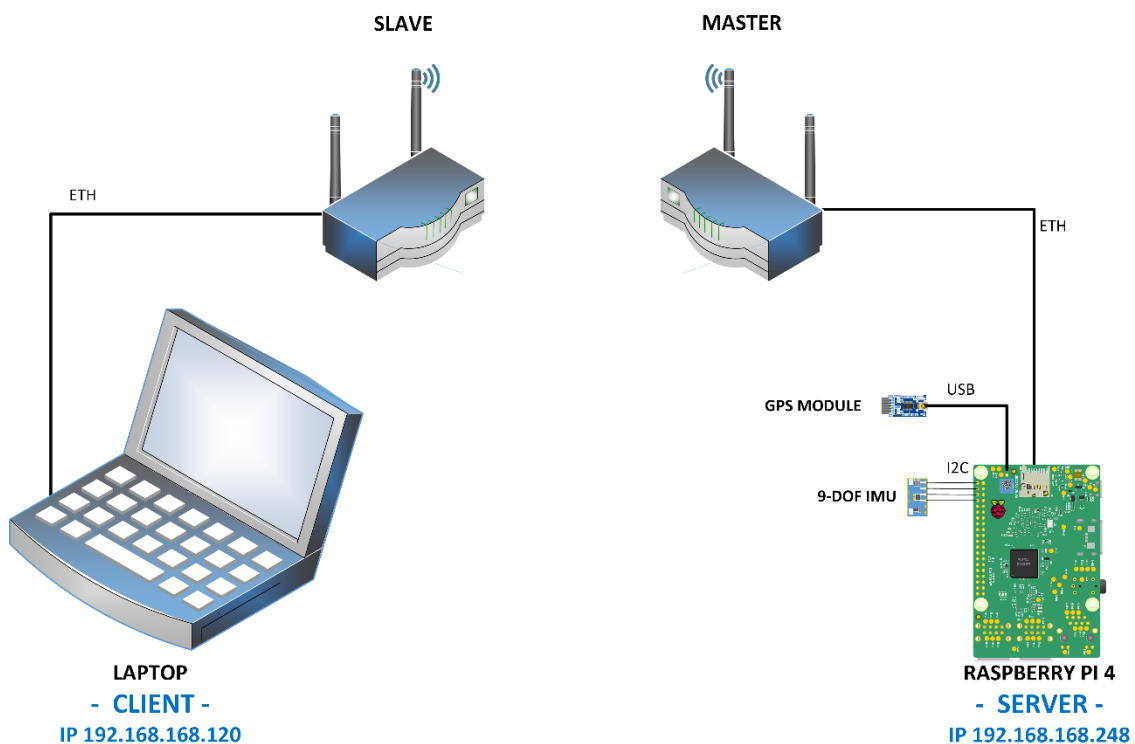


Figure 36 setup for telemetry and telecommand data exchange

To do so, a first attempt using the socket module of the python standard library was made. A socket is a software abstraction that allows two nodes on a network to communicate with each other.

A connection is made possible in this way: one socket (node) listens on a particular port at an

IP while the other socket connects to the other on the same port. This is essentially a connection between a server (the listener that awaits on a given port) and a client. In python is possible to create a socket object to establish this type of connection in this way:

```
import socket
s = socket.socket(socket.socket_family, socket.socket_type)
```

The first argument passed to the socket.socket function is the socket family. A commonly used socket family is AF\_INET, that is the IPv4 addresses.

The socket type is the type of socket to create, TCP type socket can be created using SOCK\_STREAM. After the creation of the socket on both ends (Server/Raspberry and Client/Laptop) is possible to differentiate the code.

Server code:

```
import socket
import sys
# Create a TCP/IP socket
sock = socket.socket(socket.AF_INET, socket.SOCK_STREAM)
# Bind the socket to the port
server_address = ('192.168.168.248', 60000)
sock.bind(server_address)
# Listen for incoming connections
sock.listen(1)

while True:
    # Wait for a connection
    connection, client_address = sock.accept()

    [... RECEIVE REQUEST AND SEND DATA ...]

    finally:
        # Clean up the connection
        connection.close()
```

Client code:

```
import socket
import sys
# Create a TCP/IP socket
sock = socket.socket(socket.AF_INET, socket.SOCK_STREAM)
# Connect the socket to the port where the server is listening
server_address = ('192.168.168.254', 60000)
sock.connect(server_address)
try:

    [... SEND REQUEST AND RECEIVE DATA ...]

finally:
    sock.close()
```

The server will bind on the IP '192.168.168.254' and port 60000 listening and waiting for the client to start a connection. Once the connection happens it can be possible to exchange data with the commands socket.send(DATA) and socket.recv(DATA). These functions allow to send and receive data only in bytes-object type.

This process is summarised in Figure 37, (Jennings, s.d.).

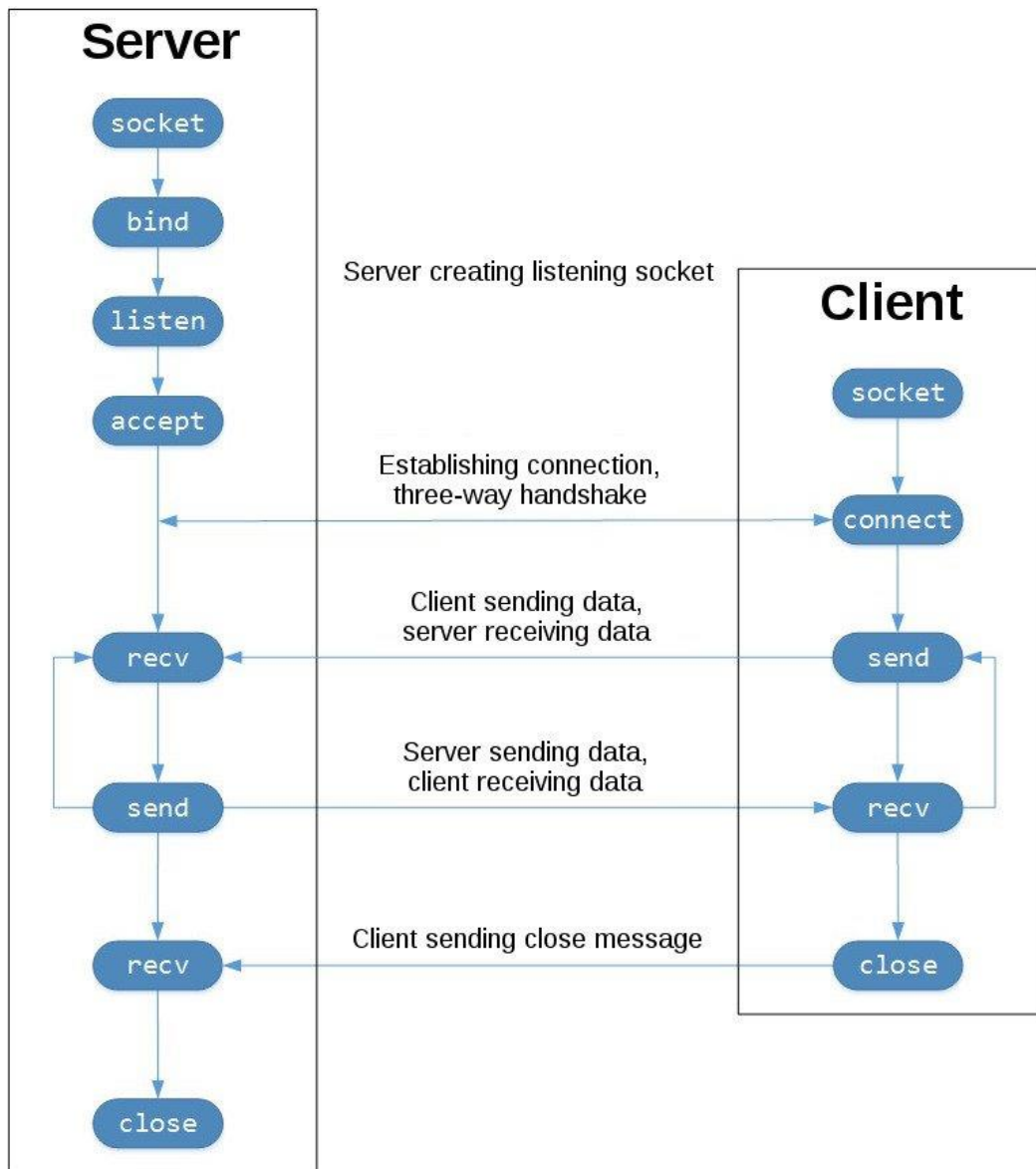


Figure 37 TCP socket flow diagram

Even though this solution is viable, it is complex to send and receive all the information in bytes format and to manage the protocol appropriately, therefore, a simpler approach is used: instead of sockets, a Message-Passing System based on sockets, is used. Message-Passing allows to send and receive messages from/to two processes in two ways:

- Asynchronous message passing: the sender sends the message and continues to perform its operations
- Synchronous message passing: the sender sends the message and waits until the receiver has received the message, processed the reply, and sent it back
- Hybrids: the sender waits until the receiver is ready to receive, and only after the receiver has made himself available to receive, the sender send the message.

Specifically, the messaging library used in this application is ZeroMQ (also known  $\emptyset$ MQ, 0MQ, zmq).

ZeroMQ, where zero imply zero broker, zero latency, zero cost and zero administration, is aimed at use in distributed or concurrent applications and is supported for many programming languages, therefore, it could still be used in the future on other platforms.

Other than its portability, as expected, it delivers messages instead of stream of bytes and it can optimize its functionality to support different messaging patterns, that are:

- Request-reply connects a set of clients to a set of services. This is a remote procedure call and task distribution pattern
- Publish-subscribe connects a set of publishers to a set of subscribers. This is a data distribution pattern
- Pipeline connects nodes in a fan-out/fan-in pattern that can have multiple steps, and loops. This is a parallel task distribution and collection pattern
- Exclusive pair connects two sockets in an exclusive pair. This is a low-level pattern for specific, advanced use cases

Each of these patterns allows the usage of different sockets that will enable the desired connection.

The request-reply pattern is designed for service-oriented architectures. And can support synchronous and asynchronous communications.

For synchronous type of messaging the socket implemented are REQ (used by a client to send requests) and REP (used by a service to receive requests and send replies to a client). The communication can happen only with the pattern send/receive/send/receive etc on the REQ socket and, conversely, on the REP socket (receive/send/receive/send etc).

For asynchronous type of messaging the usable sockets are DEALER (sends/receives messages to/from a set of anonymous peers) and ROUTER (can talk to a set of peers but addressing each message to a specific peer).

→	REQ	REP	DEALER	ROUTER
REQ		↔ S-R		↔ S-R
REP	↔ R-S		↔ R-S	
DEALER		↔	↔	↔
ROUTER	↔		↔	↔

**Table 12 summary of request-reply pattern. In green compatible peer sockets, arrow indicates directionality of the pattern**

The publish-subscribe pattern is used for distribution of data usually, but not always, from a small number of publishers to many subscribers. This pattern allows the use of topics: array of bytes sent along with the message that can tag the message's payload so that a subscriber can receive only tagged messages.

Allowed socket in this pattern are: PUB, SUB, XPUB and XSUB.

PUB is used only to send data in a fan out fashion to all connected peers. SUB is used by a subscriber to only receive data of a subscribed topic from the publisher. XPUB is analogue to

PUB with the difference that can receive a subscription message to add or remove subscribers. XSUB is analogue to SUB but it can send a subscription message.

→	PUB	SUB	XPUB	XSUB
PUB		→		→
SUB	←		←	
XPUB		→*		→*
XSUB	*←		*←	

**Table 13 summary of publish-subscribe pattern. In green compatible peer sockets, arrow indicates directionality of the pattern. \*allows to send/receive subscriptions**

The pipeline pattern is used for distribution of tasks in a multi-stage pipeline, where typically a few nodes push work to many workers, in exchange the workers push results to a few collectors. If a node disconnects suddenly the pattern will not discard messages.

The allowed sockets are PUSH and PULL. The PUSH socket type can talk to different anonymous PULL peers, it is not possible to receive on this socket.

The PULL socket receives messages from PULL socket(s), it is not possible to send on this socket.

→	PUSH	PULL
PUSH		→
PULL	←	

**Table 14 summary of pipeline pattern. In green compatible peer sockets, arrow indicates directionality of the pattern.**

Each of these patterns, implements different types of algorithms to route in and out messages (e.g. round-robin, fair-queuing, fan in, fan out, etc) and, if the limit to the maximum number of messages is reached, each socket can enter in an exceptional state that will manage the circumstance differently.

Multiple patterns were tested but publish-subscribe pattern is the one that best fits the intent of the initial testing: the raspberry will publish telemetry data and the ground station/users can access to that by subscribing.

For payload data (a Pi Camera in this case), an optimization of the same python library for images was used. The imagezmq consists in a set of python classes that can transport images elaborated with OpenCV between machines.

Zmq is especially useful, in this case, because zmq does not require a message broker, removing a step in between the hub and the peer. This means a lighter load to carry due to the absence of double handling.

Imagezmq allows only REQ/REP or PUB/SUB messaging patterns. PUB/SUB, as in the case of telemetry, is chosen as it is a non-blocking pattern for the hub (does not require a reply each time the hub sends a message).

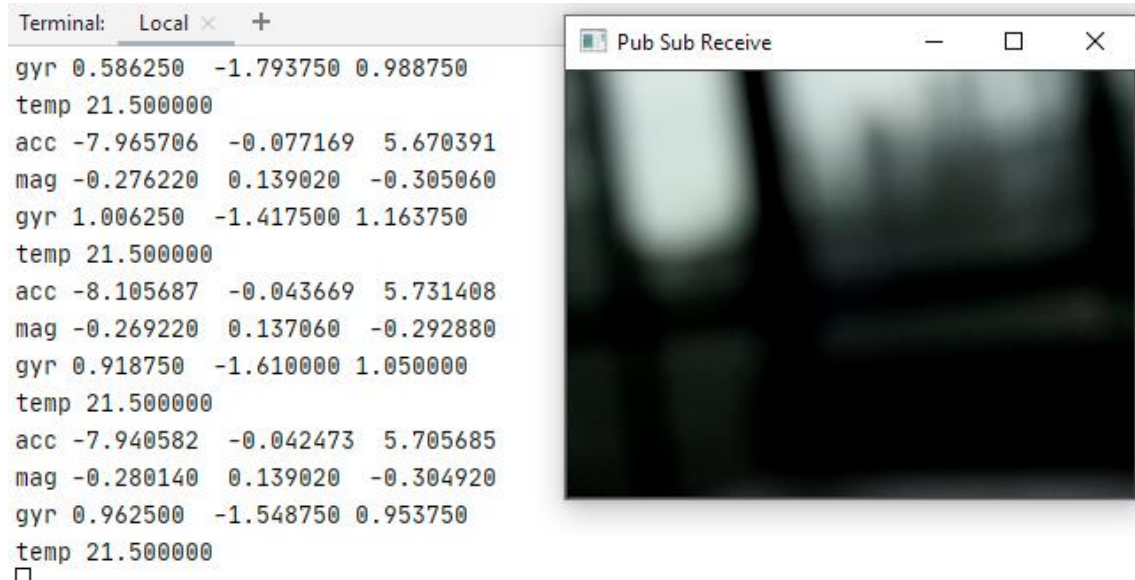


Figure 38 Receiving telemetry and payload data from the raspberry.

#### 4.2.2 Short range test results

To integrate and test the preliminary capabilities of the link, some tests were made in the surrounding area of Stratobotic's laboratory at a range of around 100 m in LOS. This test was performed to assess, apart from the battery pack ability to withstand the load, the capabilities to send and receive data without power supplies and other test equipment and to evaluate if any criticality could affect the communication between the two ends (ground station and payload prototype).

The first parameters collected were the real time RF performance of the slave transceiver evaluated with the following settings:

- *frequency 2.4 GHz*
- *Bandwidth 8MHz*
- *txPower 30 dBm* at both ends
- dipole antennas on both ends
- automatic modulation scheme selection

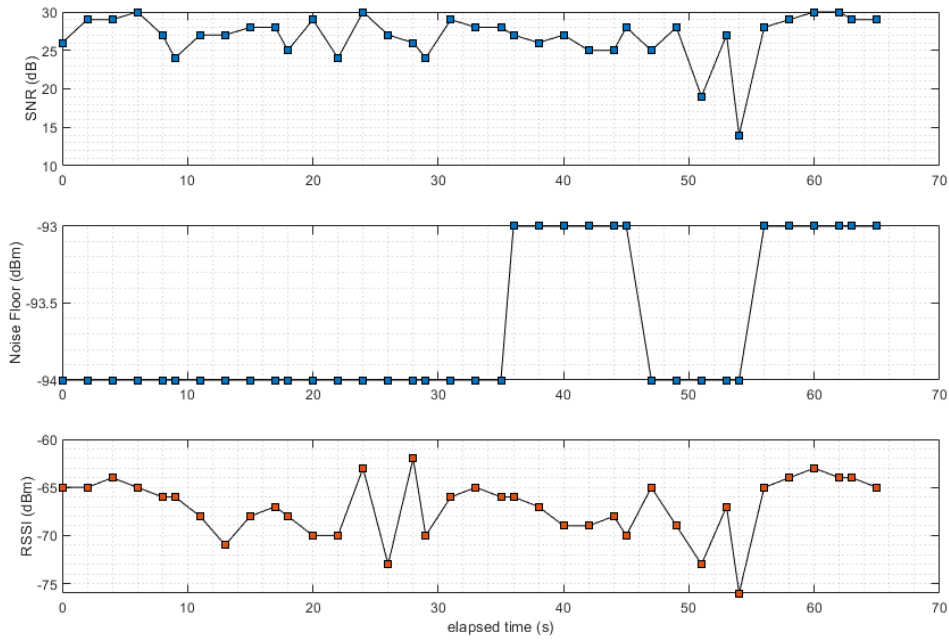


**Figure 39 RF performances in short range test**

As shown in Figure 39, the SNR was stable at around 25 dB, however using 30 dBm of tx power, it was expected to be at least 30 dBm. This discrepancy could be due to the increased noise floor with respect to the initial testing done inside the laboratory (with a delta of around 2dB), and due to electromagnetic interference.

The overall RSSI was high enough to allow 64 QAM 5/6 modulation but the limited SNR allowed only a 16 QAM 1/2 with an average throughput of around 11.0 Mbps instead of around 25 Mbps. The throughput was measured using Iperf3:

```

iperf 3.1.3
CYGWIN_NT-10.0 DESKTOP-#####
Time: Thu, 01 Apr 2021 14:49:59 GMT
Connecting to host 192.168.168.248, port 5201
[ 5] local 192.168.168.120 port 63771 connected to 192.168.168.248
port 5201
Starting Test: protocol: TCP, 1 streams, 131072 byte blocks, omitting
0 seconds, 60 second test
[ ID] Interval            Transfer       Bandwidth
[ 5]  0.00-1.01    sec  1.62 MBytes  13.6 Mbits/sec
[ 5]  1.01-2.01    sec  1.50 MBytes  12.6 Mbits/sec
[ 5]  2.01-3.01    sec  1.12 MBytes  9.37 Mbits/sec
[ 5]  3.01-4.00    sec  1.38 MBytes  11.7 Mbits/sec
[ 5]  4.00-5.00    sec  1.12 MBytes  9.44 Mbits/sec
[ 5]  5.00-6.01    sec  1.38 MBytes  11.5 Mbits/sec
[ 5]  6.01-7.01    sec  1.50 MBytes  12.5 Mbits/sec
[ 5]  7.01-8.01    sec  1.25 MBytes  10.5 Mbits/sec
[ 5]  8.01-9.01    sec  1.50 MBytes  12.7 Mbits/sec
[ 5]  9.01-10.01   sec  1.00 MBytes  8.36 Mbits/sec
[ 5] 10.01-11.00   sec  1.00 MBytes  8.45 Mbits/sec
[. . .]
[ 5] 59.01-60.01   sec  1.50 MBytes  12.5 Mbits/sec
-----
Test Complete. Summary Results:
[ ID] Interval            Transfer       Bandwidth
[ 5]  0.00-60.01   sec  78.4 MBytes  11.0 Mbits/sec
sender
[ 5]  0.00-60.01   sec  78.3 MBytes  11.0 Mbits/sec
receiver
CPU Utilization: local/sender 0.3% (0.1%u/0.2%s), remote/receiver 6.1%
(0.4%u/5.8%s)

iperf Done.

```

The mismatch in the measured and the expected performances is suspected to be produced by the noise and reflections of the urban environment and, in general, by the reduced clearance that was available during the test.

This might have caused the unsatisfaction of the Fresnel Zone, therefore the inability to transmit at the maximum throughput.

After taking those measures, the telemetry data was retrieved successfully. It consists of: TIMESTAMP, GNSS LONGITUDE, GNSS LATITUDE, GNSS ALTITUDE, ACCELERATION ALONG X, ACCEL ALONG Y, ACCEL ALONG Z, MAGNETIC FIELD ALONG X, M F ALONG Y, M F ALONG Z, ROTATION ALONG X, ROTATION ALONG Y, ROTATION ALOG Z, AVERAGE TEMPERATURE.

```
Connecting to server 192.168.168.248 : 60000
Fix timestamp: 4/1/2021 14:53:06, 45.091792, 7.661625, 227.100000, -
1.575674, 1.541576, 9.269795, -0.252140, 0.281260, -0.474880,
6.947500, 0.035000, 5.538750, 26.500000
Fix timestamp: 4/1/2021 14:53:06, 45.091792, 7.661625, 227.100000, -
1.140180, 1.300499, 9.340981, -0.092540, 0.488740, -0.554540, -
13.300000, -29.190000, -90.142500, 25.500000
Fix timestamp: 4/1/2021 14:53:07, 45.091792, 7.661625, 227.100000, -
0.689133, 2.992823, 9.067003, -0.247940, 0.291900, -0.481180, -
9.301250, 3.718750, -17.412500, 26.500000
Fix timestamp: 4/1/2021 14:53:07, 45.091792, 7.661625, 227.100000, -
1.596013, 2.844468, 8.949157, -0.270620, 0.270340, -0.455700, -
3.613750, -4.392500, -0.201250, 25.500000
Fix timestamp: 4/1/2021 14:53:08, 45.091790, 7.661627, 227.100000, -
2.451447, 2.967100, 9.012566, -0.292740, 0.261100, -0.454020, -
3.307500, 1.417500, 5.337500, 25.500000
Fix timestamp: 4/1/2021 14:53:08, 45.091790, 7.661627, 227.100000, -
2.907279, 3.237489, 8.712865, -0.288260, 0.237860, -0.444500,
3.298750, -6.282500, -17.386250, 26.500000
Fix timestamp: 4/1/2021 14:53:09, 45.091790, 7.661627, 227.100000, -
2.099104, 3.373282, 8.661420, -0.278180, 0.248780, -0.439040,
0.096250, 0.420000, 2.528750, 26.500000
Fix timestamp: 4/1/2021 14:53:09, 45.091790, 7.661627, 227.100000, -
2.334797, 2.941975, 8.755936, -0.272860, 0.200340, -0.429100,
2.292500, -5.670000, 7.358750, 26.500000
Fix timestamp: 4/1/2021 14:53:10, 45.091790, 7.661628, 227.100000, -
2.286940, 2.659024, 8.888140, -0.267260, 0.193620, -0.423080,
0.000000, 0.306250, 11.138750, 26.500000
```

During the test, the payload data was also set to be collected, however due to a failure in the code, the camera captured only black images.

### 4.3 Outdoor testing

To evaluate the in-flight performances achievable with the Microhard pMDDL5824, outdoor testing shall be considered to assess how different parameters can affect the link budget. These tests are extremely important because they can highlight potential issues at various levels: logistics, RF performances, electronics performances, hazards and so on.

For the purpose of this work the main parameters to investigate are those which can affect the RF performances and, in short, the throughput.

### 4.3.1 Selection of suitable antennas

The Microhard pMDDL5824 operates at two main frequencies that are 2.4 GHz and 5.8 GHz and it comes with two dual-band omni directional whip antennas with SMA female connectors. Whip antennas are commonly designed as resonant antennas where the rod acts as a resonator for radio waves. Therefore, the length of the antenna rod is determined by the wavelength of the radio waves used. The most common length is about a quarter of a wavelength, called a quarter-wave whip but half-wave whips are also used.

The radiation pattern of a whip antenna, usually, is a toroidal pattern with maximum gain between 3 and 6 dBi, but its shape can change based on its electrical length. An example of a 2.4 GHz monopole radiation pattern for an antenna at  $\lambda/2$  is shown in Figure 40

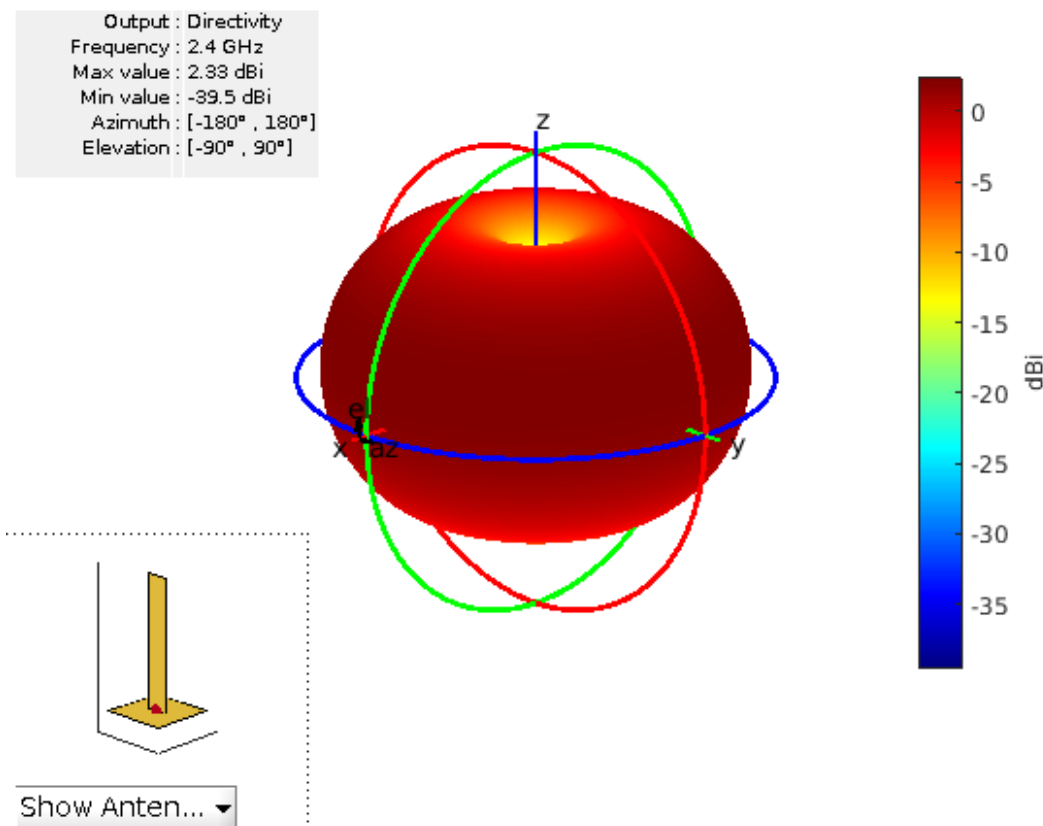


Figure 40 Radiation pattern of a  $\lambda/2$  2.4 GHz whip antenna

Even though these antennas are compact and versatile they can allow communications only for few kilometres.

In fact, to quickly evaluate the link capabilities, a basic formula can be used:

$$\text{Fade Margin} = \text{System Gain} - \text{Path Loss} > 10 \div 20 \text{ dB}$$

where

$$\text{SystemGain} = \text{TxPower} + (\text{TxGain} - \text{TxLoss}) + (\text{RxGain} - \text{RxLoss}) + |\text{RxSensitivity}|$$

The pMDDL5824 maximum Tx Power is 30 dBm, the Rx Sensitivity for maximum performances is -78 dBm (however it can be lowered at the expense of data rate), assuming 1 dB of loss both in the Tx and Rx side and 3 dB of Tx and Rx gain, then the Fade Margin for different modulation schemes at 2.4 GHz and for a 8 MHz channel is shown in Figure 41.

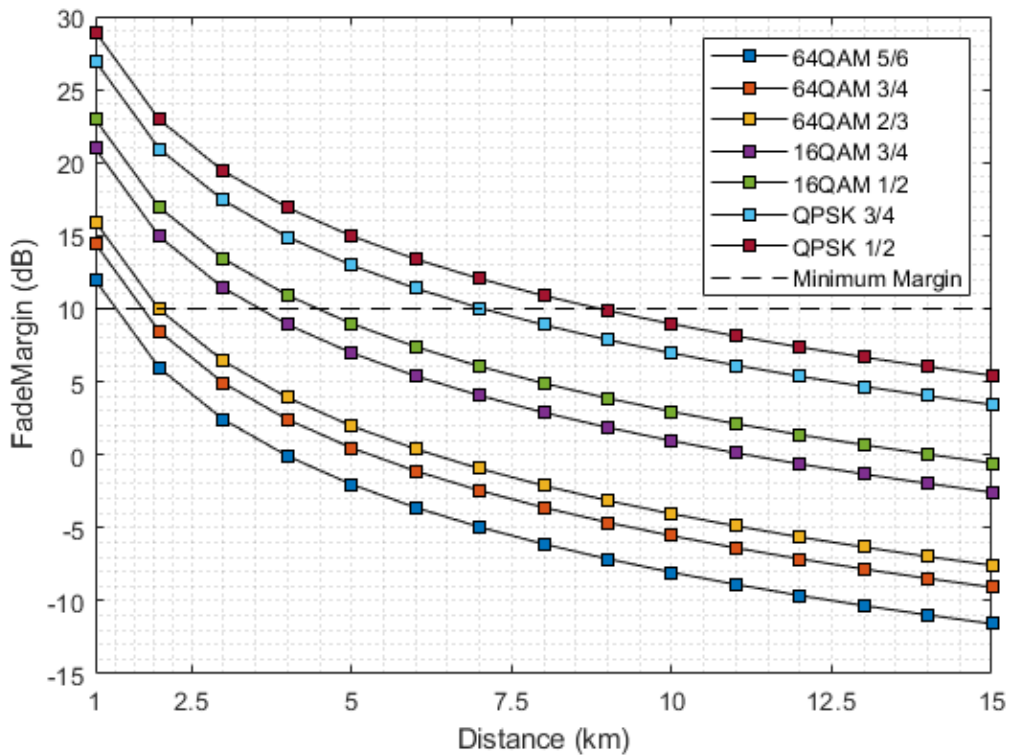


**Figure 41** Fade Margin variation with distance at 2.4 GHz in a 8MHz channel for the Microhard pMDDL5824

It is clear that dipole antennas can allow reliable, fast (> 20Mbps) communication links only at a distance of less than 2.5 km while, reducing the throughput at its minimum (i.e. less than 3 Mbps enabling QPSK ½ on a 4 MHz or narrower channel), links up to 8-10 kilometres can be closed.

To increase the System Gain, therefore the Fade Margin, the only degrees of freedom are the Tx and Rx antenna Gains (as the Tx Power and the Rx Sensitivity are dictated by the pMDDL5824 and can only be increased using external amplifiers).

Using directional antennas can increase the range at which is possible to have a high-throughput communication link, however, it should be noted that, increasing the directivity will increase the gain but will lower the beamwidth, exposing the system to misalignment. Antenna misalignment means that the received signal is not received at the peak of the antenna beam and/or the portion of transmitting a signal that is received did not come from the peak of the transmit antenna beam. This is a major issue when very high gain antennas are used (e.g. parabolic

dishes) while communicating with moving targets because aligning the Tx and Rx beams will require accurate tracking.

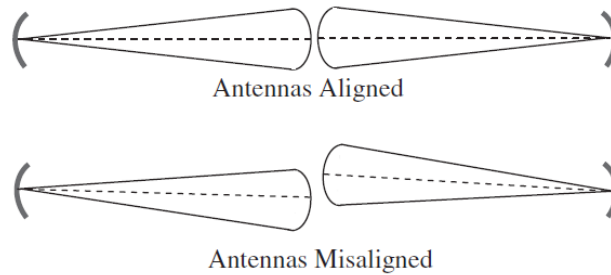


**Figure 42 Antenna alignment and misalignment for a point-to-point link using directional antennas**

Pointing loss can happen in diverse ways. The initial antenna alignment is hardly perfect; on a point-to-point link, each end must be aligned. Besides, effects such as wind, age, and thermal effects may all contribute to changing the antenna alignment over time. Variation in atmospheric refraction can produce time-varying pointing error, which can be challenging to identify.

The pointing error loss can be calculated as:

$$L_{\theta} = -12 \left( \frac{e}{\theta} \right)^2$$

where  $\theta$  is the 3 dB beamwidth in degrees and  $e$  is the pointing offset in degrees.

For medium range communication links, a good trade-off between gain and beamwidth can be obtained using panel, Yagi or patch antennas:

- Panel antennas consists of a dipole paced ahead of a metal panel reflector; it is a very simple way to increase the overall gain of the system to 8-15 dBi along one plane. The beamwidth its usually large 30-60° In the horizontal plane, while the vertical beam stays around 15 degrees.
- Yagi (also called Yagi-Uda) antennas are simple directional antennas consisting of a driven dipole and a series of parallel metal rods that act as resonant elements to direct the beam in one direction. As it consists of dipoles it can be used for linearly polarized signals. The gain of such antennas can range from 10 to 25 dBi depending on the geometry, the half power beamwidth can range from 50 to 20 degrees.
- Patch (or microstrip) antennas consists of “patch” of metal mounted over a larger metal panel, the two form a resonant transmission line. A single patch antenna can provide a gain of around 6-9 dBi in a wide beam, however, multiple patch antennas on the same substrate can be used to make high gain array antennas (called microstrip antennas) and phased arrays in which the beam can be electronically steered, in this case those antennas can be used to support MIMO techniques.

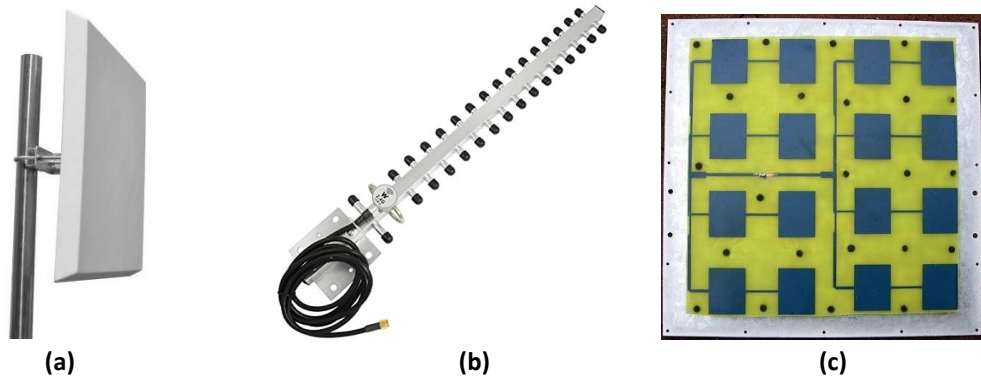


**Figure 43** Examples of panel (a), Yagi (b) and Microstrip (c) antennas

Very high gain antennas can be used to establish a communication link over very long distances ( greater than 20-30 km) such as parabolic dishes but as the half power beamwidth can then range from 2 to 10 degrees, depending on the reflector geometry, the system will need very precise tracking with a mechanical and/or electronic control loops to align the Tx and Rx beams to avoid heavy pointing error losses.

### 4.3.2 Simulations

The experiment involves two transceivers, one placed on top of Superga hill, and the other one at Stratobotic laboratory, in Turin, which has a direct view of the hill, therefore, a LOS communication link can be established. This setup can be used as reference for future in-flight tests and to assess the behaviour of a real data link at a range of about 8.3 km and to assess the battery pack performances.

This setup is also useful to evaluate the goodness of the models used so far, in particular, the Matlab and STK models.

An STK simulation is, therefore, prepared:

- To simulate the link geometry, the local digital elevation model (SRTM in particular) has been retrieved from ([earthexplorer, s.d.](#))
- A transmitter with 30 dBm Tx power is placed at the edge of Superga hill, 15 m above the ground and a receiver at Stratobotic laboratory placed at the same height.
- As the transceivers are identical, only a one-way link is simulated
- Different antenna configurations are evaluated: Dipole to Dipole, Yagi to Dipole and Yagi to Yagi. The dipole is at  $\lambda/2$  and the Yagi is supposed to have 15 dB gain.



**Figure 44 Simulation of the outdoor test at Superga hill**

Azimuth and Elevation angles from the laboratory to Superga are:  $AZ = 98.5^\circ$ ;  $EL = 2.9^\circ$ .

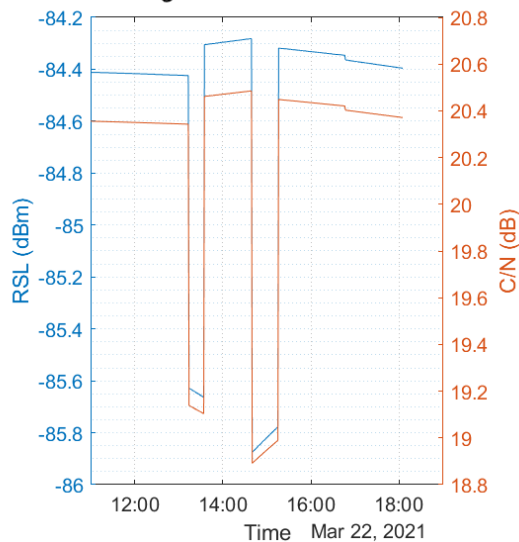
Results are shown in the following page. The RSL can be compared directly to the Throughput @ Sensitivity specified by the manufacturer, in this case at MIMO OFF:

<b>MIMO OFF</b>			
<b>Modulation</b>	<b>IPerf Throughput (Mbps)</b>	<b>Throughput @ Sensitivity (dBm)</b>	<b>Maximum Total Tx Power (dBm) +/- 1dB</b>
<i>8 MHz Channel Bandwidth</i>			
QPSK_1/2	5.8	-95	30 dBm
QPSK_3/4	8.6	-93	30 dBm
16QAM_1/2	11.5	-89	30 dBm
16QAM_3/4	16.9	-87	30 dBm
64QAM_2/3	22.2	-82	28 dBm
64QAM_3/4	24.7	-80.5	28 dBm
64QAM_5/6	27.4	-78	27 dBm

**Table 15 Microhard pMDDL5824 performance specification @ maximum bandwidth and MIMO OFF**

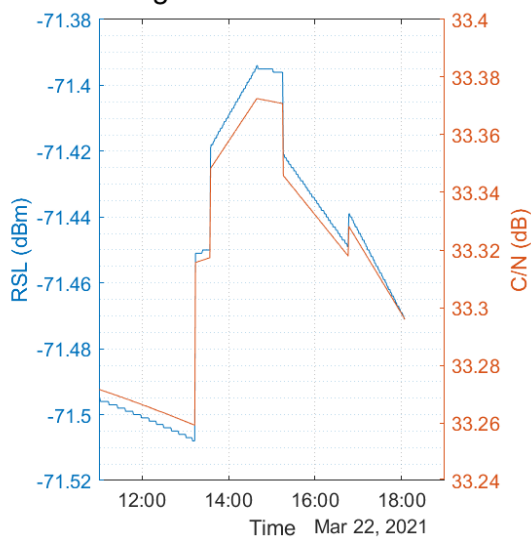
### DipoleToDipoleLink Budget

Parameter	Value	Units
Frequency	2.4000	GHz
Range	8.3571	km
Cumulative Loss	118.5622	dB
Channel Bandwidth	8.3330	MHz
Transmitted Power	30	dBm
tx Antenna Gain	2.1184	dBi
EIRP	2.1185	dBw
rx Antenna Gain	2.1489	dBi
G/T	-22.7332	dB/K
Eb/N0 Threshold	10	dB
Avg. Link Margin	5.4427	dB



### YagiToDipoleLink Budget

Parameter	Value	Units
Frequency	2.4000	GHz
Range	8.3571	km
Cumulative Loss	118.5622	dB
Channel Bandwidth	8.3330	MHz
Transmitted Power	30	dBm
tx Antenna Gain	15	dBi
EIRP	15	dBw
rx Antenna Gain	2.1486	dBi
G/T	-22.5145	dB/K
Eb/N0 Threshold	10	dB
Avg. Link Margin	18.5431	dB



### YagiToYagiLink Budget

Parameter	Value	Units
Frequency	2.4000	GHz
Range	8.3571	km
Cumulative Loss	118.5622	dB
Channel Bandwidth	8.3330	MHz
Transmitted Power	30	dBm
tx Antenna Gain	15	dBi
EIRP	15	dBw
rx Antenna Gain	15	dBi
G/T	-9.6497	dB/K
Eb/N0 Threshold	10	dB
Avg. Link Margin	31.4078	dB

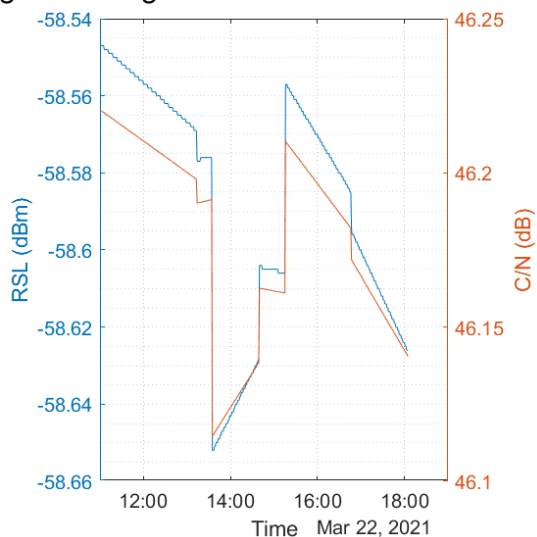


Figure 45 Simulated results for a Superga-Turin link with Microhard pMDDL5824 using different antennas

From the results can be noted that the oscillation in the RSL is greater if a dipole is used in the communication link. This is because the dipole is set to a fix orientation while the Yagi, in the model used, can track its target.

That said, this link should provide at least 16.9 Mbps of throughput with dipole antennas (16QAM with 3/4 FEC) while it should work at maximum performances in the other two configurations: 27.4 Mbps (64QAM with 5/6 FEC).

## 5 Conclusions and future developments

This work summarises the activities carried out for and with Stratobotic s.r.l which was focused on three main points: to provide realistic link budgets for HAPS telecommunication missions; to design a flexible and re-configurable payload to support such missions and, finally, to provide support to the configuration and testing phase of the Microhard pMDDL5824.

Link budgets were evaluated mainly for dedicated missions in support of maritime cruises in C band and as an aid to geostationary satellite internet connectivity in Ka band. Such links have been analysed mainly with Matlab and AGI STK, however, to validate the results, it should be considered to analyse the same links with other tools.

For the future, investigations at higher frequencies should be evaluated to assess the capabilities and the limits of light platforms in such conditions. Furthermore, as this work was focused in great part on point-to-point communications, extending it to point-to-multipoint analyses could produce helpful results for real data links. In addition to that, as the goal of Stratobotic, is to deploy a large number of such lightweight platforms to form constellations of HAPS, interlink communication capabilities should be evaluated in the future.

To design the telecommunication payload great resonance was given to its capability of being re-configurable, therefore an SDR-based architecture has been chosen amongst other analogue architectures. However, given the youthfulness of the project, the mission could change anytime from a multi-service oriented platform to a single or limited-service oriented one. In such a case, designing (or using a commercial) analogue payload could be the best option to save cost, but more importantly, on-board power and mass.

To design the RF layer of the payload, references were taken from simple and commonly used devices. However, being a prototype design, obtained from high-level requirements and key drivers and not from a specification, it is far from being optimal. After the initial stages, when the mission will turn on specific services and highlight explicit performance parameters, a second iteration of design could produce a more complete result.

The simulation will stay relevant and, to validate its results, it should be compared against other widely used dedicated tools such as Keysight ADS for the components of RF layer and SystemVue for the entire digital communication link.

In the last part of this thesis work, a multi-purpose commercial transceiver was configured and tested. As part of the test plan, telemetry and payload data have been successfully transmitted and received indoor, while some issues were spotted during the short-range tests. The signal strength was measured to be lower than expected thus, further analyses are required to understand the origin of the inconsistency. It is recommended to perform the same test in an open space with adequate clearance (the obstruction-free area should be much greater than the physical LOS) and with the transceivers placed at an elevation above ground of at least 5 meters.

## Bibliography

- [1] (n.d.). Retrieved from nuand: <https://www.nuand.com/product/bladeRF-xA9>
- [2] Book by Dale S W Atkinson, K. W. (2015). *Software-Defined Radio Using MATLAB, Simulink, and the RTL-SDR*. Strathclyde Academic Media.
- [3] David Large, J. F. (2003). *Modern Cable Television Technology*. Morgan Kaufmann. Retrieved from <https://www.sciencedirect.com/topics/engineering/bit-error-rate>
- [4] E. Galanaki, K. L. (2018). Thunderstorm climatology in the Mediterranean using cloud-to-ground lightning observations. 10.
- [5] *earthexplorer*. (n.d.). Retrieved from <https://earthexplorer.usgs.gov/>
- [6] Eutelsat Archived Communications. (2008). *web.archive.org*. Retrieved from <https://web.archive.org/web/20080618181945/http://www.eutelsat.com/satellites/upcoming-launches.html>
- [7] [frequencyplansatellites.altervista.org](http://frequencyplansatellites.altervista.org/). (n.d.). <http://frequencyplansatellites.altervista.org/>. Retrieved from [http://frequencyplansatellites.altervista.org/Eutelsat/Eutelsat\\_KaSat\\_9A.pdf](http://frequencyplansatellites.altervista.org/Eutelsat/Eutelsat_KaSat_9A.pdf)
- [8] <https://www.electronics-notes.com>. (n.d.). Retrieved from <https://www.electronics-notes.com/articles/radio/modulation/quadrature-amplitude-modulation-what-is-qam-basics.php>
- [9] IEEE. (n.d.). Retrieved from <http://www.classic.grss-ieee.org/>: [http://www.classic.grss-ieee.org/frequency\\_allocations.html](http://www.classic.grss-ieee.org/frequency_allocations.html)
- [10] International Telecommunication Union - Radiocommunication Sector. (2019). World Radiocommunication Conference 2019 - Final Acts. *WRC-19*. Sharm El-Sheikh.
- [11] ITU-R P.618. (2017). *Propagation data and prediction methods required for the design of Earth-space telecommunication systems*.
- [12] ITU-R P.838-3. (2005). *Specific attenuation model for rain for use in prediction methods*.
- [13] ITU-R P.840-6. (2013). *Attenuation due to clouds and fog*.
- [14] Jennings, N. (n.d.). *realpython*. Retrieved from <https://realpython.com/python-sockets/>
- [15] Keysight Technologies. (2010). *Fundamentals of RF and Microwave Noise Figure Measurements*. Agilent.
- [16] *pasternack*. (n.d.). Retrieved from <https://www.pasternack.com/>
- [17] *pasternack*. (n.d.). Retrieved from pasternack: <https://www.pasternack.com/40-db-gain-6-ghz-low-noise-high-gain-amplifier-sma-pe15a1010-p.aspx>
- [18] Recommendations, ITU-R. (1999). *Attenuation due to clouds and fog*. Geneva: ITU-R P.840-3.
- [19] Seybold, J. S. (2005). *Introduction to RF Propagation*. Wiley.
- [20] Sheetz, M. (2020, 10 27). Retrieved from [cnn.com/2020/10/27/spacex-starlink-service-priced-at-99-a-month-public-beta-test-begins.html](https://www.cnn.com/2020/10/27/spacex-starlink-service-priced-at-99-a-month-public-beta-test-begins.html)
- [21] skylogic. (2012). *skylogic.it*. Retrieved from <https://www.skylogic.it/eutelsat-sets-a-new-benchmark-for-satellite-broadband-via-ka-sat/>
- [22] Werner, D. (2020, November 19). *Spacenews*. Retrieved from [www.spacenews.com: https://spacenews.com/viasat-claims-ka-sat/](https://spacenews.com/viasat-claims-ka-sat/)
- [23] Westgarth, A. (2021, January 22). Retrieved from [medium.com: https://medium.com/loon-for-all/loon-draft-c3fceb11f3f](https://medium.com/loon-for-all/loon-draft-c3fceb11f3f)
- [24] *wikipedia*. (n.d.). Retrieved from [https://en.wikipedia.org/wiki/List\\_of\\_software-defined\\_radios](https://en.wikipedia.org/wiki/List_of_software-defined_radios)
- [25] [www.minicircuits.com](http://www.minicircuits.com). (n.d.). Retrieved from <https://www.minicircuits.com/WebStore/dashboard.html?model=BFCV-4085%2B>